Molecular Mechanism of Metaphase-? Arrest in Mouse Oocytes

Molecular Mechanism of Metaphase-II Arrest in Mouse Oocytes

January 2014

Yu Miyagaki

Molecular Mechanism of Metaphase-II Arrest in Mouse Oocytes

A Dissertation Submitted to

the Graduate School of Life and Environmental Sciences,

the University of Tsukuba

in Partial Fulfillment of the Requirements

for the Degree of Doctor of Philosophy

(Doctoral Program in Life Science and Bioengineering)

Yu MIYAGAKI

CONTENTS

GENERAL INTRODUCTION

Vertebrate oocytes are arrested at prophase of meiosis I and undergo maturation after hormonal stimulation (Kishimoto, 2003; Sagata, 1996). The mature oocytes are rearrested at metaphase of meiosis II until fertilization. The metaphase-II arrest is characterized by high kinase activity of Cdk1-cyclin B complex, maturation promoting factor MPF, that prevents parthenogenetic activation (Perry and Verlhac, 2008; Tunquist and Maller, 2003).

Emi2 is known to be a direct inhibitor of the anaphase-promoting complex/cyclosome (APC/C) required for degradation of cyclin B, and to cause metaphase-II arrest (Madgwick et al., 2006; Schmidt et al., 2005; Shoji et al., 2006; Tung et al., 2005). In *Xenopus*, Mos-MAPK pathway (Mos-Mek1/2-Erk1/2-Rsk1/2/3) is involved in metaphase-II arrest through phosphorylation of Emi2 (Inoue et al., 2007; Nishiyama et al., 2007). Rsks possess the ability to phosphorylate four Ser/Thr residues of Emi2 at positions S335, T336, S342, and S344. Multiple phosphorylation of Emi2 is required for its stability and inhibitory binding to the APC/C, thereby promoting the metaphase-II arrest.

In mice, other kinase pathways may be involved in phosphorylation of EMI2, because the oocytes lacking three RSKs, RSK1, RSK2, and RSK3, exhibit the normal metaphase-II arrest (Dumont et al., 2005). Moreover, inhibition of MEK1/2 synthesis by siRNA has little on metaphase-II arrest (Yu et al., 2007). In this study, I examined whether MSK1 and p38 play a key role in the metaphase-II arrest through phosphorylation of EMI2.

CHAPTER I

Possible involvement of mitogen- and stress-activated protein kinase 1, MSK1, in metaphase-II arrest through phosphorylation of EMI2 in mouse oocytes.

SUMMARY

Ovulated oocytes are arrested at the metaphase of second meiotic division. The metaphase-II arrest in *Xenopus* oocytes is regulated by RSKs located downstream of the Mos‐MAPK pathway. In mice, other kinase(s) besides RSKs may be responsible for the metaphase-II arrest, because RSK1/RSK2/RSK3-triple knockout mice exhibit no obvious phenotype. Here, I show the subcellular localization and possible role of mitogen- and stress-activated kinase 1, MSK1 known as another downstream kinase of the Mos‐MAPK pathway, in the mouse oocyte. Immunostaining analysis indicated that MSK1 is present in the germinal vesicle (GV) and cytoplasm of oocytes at the GV and metaphase-II stages, respectively. An active, phosphorylated form of MSK1 was predominantly localized to the metaphase-II spindle. The inhibition of the MSK1 activity failed to maintain the sister chromatid alignment within the metaphase-II plate. Importantly, MSK1 exhibited the ability to phosphorylate four Ser/Thr residues of meiotic cell-cycle regulator EMI2. The phosphorylation was required for up-regulation of the EMI2 activity in the oocytes. These results suggest that mouse MSK1 may play a key role in the metaphase-II arrest through phosphorylation of EMI2.

INTRODUCTION

The meiotic cell cycle consists of two successive divisions: meiosis I and meiosis II. Germinal vesicle (GV)-stage oocytes in many vertebrates are arrested first at the prophase of meiosis I and undergo maturation after hormonal stimulation (Kishimoto, 2003; Sagata, 1996). The mature oocytes are re-arrested by cytostatic factor CSF at the metaphase of meiosis II (Masui and Markert, 1971). The metaphase-II arrest of the oocytes is regulated by the Mos–MAPK pathway that maintains the kinase activity of CDK1–cyclin B complex (maturation promoting factor, MPF) at an elevated level (Perry and Verlhac, 2008; Tunquist and Maller, 2003). Following fertilization the kinase activity of MPF is reduced owing to degradation of cyclin B, which leads to release from the metaphase-II arrest of the oocytes.

F-box protein 43 (EMI2), a key component of CSF, is known to inhibit anaphase-promoting complex/cyclosome (APC/C) required for degradation of cyclin B, and to cause the metaphase-II arrest in the mouse and *Xenopus* oocytes (Madgwick et al., 2006; Schmidt et al., 2005; Shoji et al., 2006; Tung et al., 2005). Both stability and activity of *Xenopus* Emi2 in the metaphase-II arrest are up-regulated by RSKs, 90-kDa ribosomal S6 kinases, located immediately downstream of ERK1/2 MAPK (Bhatt and Ferrell, 2000; Gross et al., 2000; Inoue et al., 2007; Nishiyama et al., 2007). RSKs possess the ability to phosphorylate four Ser/Thr residues of *Xenopus* Emi2 at positions S335, T336, S342, and S344. Although RSKs are identified as the ERK1/2 substrates (Kalab et al., 1996), the mouse oocytes lacking three RSKs, RSK1, RSK2, and RSK3,

exhibit the normal metaphase-II arrest (Dumont et al., 2005). Thus, these findings raise the possibility that other kinase(s) instead of RSKs may participate in phosphorylation of EMI2 in the mouse oocytes (Inoue et al., 2007; Suzuki et al., 2010).

Mitogen- and stress-activated protein kinases, MSK1 and MSK2 (RPS6KA5 and RPS6KA4, respectively), are activated by ERK1/2 and/or p38 MAPK following cellular stimulation in somatic cells (Deak et al., 1998; Pearce et al., 2010; Wiggin et al., 2002). MSKs resemble RSKs because these proteins belong to the AGC kinase subfamily, and have two kinase domains connected by a regulatory linker region. However, the presence and function of MSKs in the mouse oocytes still remain uncertain. In this study, I have focused on the subcellular localization and function of MSK1 in the mouse oocytes. My data suggest that MSK1 may play a key role in phosphorylation of EMI2 to maintain the metaphase-II arrest.

MATERIALS AND METHODS

Plasmids

DNA fragments encoding EMI2 (GenBank ID: NP_001074772.1), MSK1 (GenBank ID: AAQ24165.1), and CREB (GenBank ID: NP_034082.1) were amplified by PCR using a mouse ovary or testis cDNA library as a template. The following sets of oligonucleotides were used as primers: 5′-GGGCGGCCGCGGATGGACTCCTCTGCTGTC-3′ and 5′-GGCTCGAGTCAGAGGCGTTTTAAGTTCCGC-3′ for EMI2; 5′-GCCTCGAGAGGGTGAAGATGGAGGG-3′ and 5′-GCTCTAGAACATACCTCAGGCACATG-3′ for MSK1; 5′-GCGAATTCATGACCATGGAATCTGGAGC-3′ and 5′-GCCTCGAGAACTTAAATCCCAAATTAATC-3′ for CREB. The amplified fragments were introduced into pcDNA3/FLAG-HA or pGEX-4T-1. To prepare pET-32a/EMI2, pGEX-4T-1/EMI2, and pGEX-4T-1/EMI2 plasmids containing the EMI2 sequences at residues 3–400, 3–400, and 204–383, respectively, DNA fragments were PCR-amplified from pcDNA3/FLAG-HA/EMI2 as a template, and introduced into the vectors. pcDNA3.1-poly(A)/FLAG-HA/EMI2 plasmid was prepared by introducing the *Kpn*I/*Bam*HI fragment of pcDNA3/FLAG-HA/EMI2 into pcDNA3.1-poly(A), as described previously (Yamazaki et al., 2007). In vitro site-directed mutagenesis was carried out according to the manufacturer′s protocol (Agilent Technology, Santa Clara, CA).

Reverse transcription-PCR

First-strand cDNA was synthesized from total RNA of mouse oocytes using a SuperScript™ III First-Strand Synthesis system (Invitrogen, Carlsbad, CA). DNA was amplified by PCR using an Advantage cDNA Polymerase Mix (Clontech, Mountain View, CA). The following sets of oligonucleotides were used as primers: 5′-GCTACTAACTGGAGCATCTCCTTTC-3′ and 5′-TCAAGAGACGCTGAAGTAGGTCTT-3′ for MSK1; 5′-GAGATGTTCACTCACCTCTACCAG-3′ and 5′-TGAGTCAAGTAAGACGTTCTCCAG-3′ for MSK2; 5′-AAAAGCTTGGCGCTTTTGACTCAGGA-3′ and 5′-GGAATTCAAGTCAGTGTACAGGCCAG-3′ for ACTB (β-actin). The reaction program consisted of 40 cycles of 94 °C for 30 s, 62 °C for 30 s, and 68 °C for 45 s.

Antibodies

His-tagged recombinant protein of mouse EMI2 containing the amino acid sequence at positions 3–400 was produced in *Escherichia coli* BL21 (DE3), as described previously (Kim et al., 2005; Shoji et al., 2006). The recombinant protein was purified on a Ni-NTA His column (Novagen, Madison, WI), emulsified with Freund's complete (Difco Laboratories, Detroit, MI) or incomplete adjuvant (Wako, Osaka, Japan), and injected into female New Zealand White rabbits (SLC, Shizuoka, Japan). Anti-EMI2 antibody was

purified on a Sepharose 4B column previously coupled with glutathione *S*-transferase (GST)-tagged EMI2, as described previously (Baba et al., 1994). Anti-cyclin B1, anti-phosphorylated MSK1, and anti-phosphorylated ERK1/2 antibodies were purchased from Cell Signaling Technology (Danvers, MA), and anti-ACTB and anti-TUBB1 (β-tubulin) antibodies were from Sigma-Aldrich (Saint Louis,MO). Anti-MSK1 monoclonal (Cell Signaling Technology) and polyclonal (Santa Cruz Biotechnology, Santa Cruz, CA) antibodies were mainly used for immunoblot and immunostaining analysis, respectively. Horseradish peroxidase-conjugated antibodies against mouse, rat, or rabbit IgG were purchased from Jackson Immunoresearch Laboratories (West Grove, PA). Alexa Fluor 488- or 568-conjugated antibodies against rat, mouse or rabbit IgG were purchased from Molecular Probes (Eugene, OR). All animal experiments were performed ethically, and experimentation was in accord with the Guide for the Care and Use of Laboratory Animals at University of Tsukuba.

Oocyte collection and microinjection

The GV-stage oocytes were collected from ovaries of 8- to 9-week-old ICR mice (SLC) 46–48 h after intraperitoneal injection of pregnant mare's serum gonadotropin (Aska Pharmaceutical, Tokyo, Japan). The oocytes were put in a drop of KSOM (Lawitts and Biggers, 1993) containing 10 mM HEPES and 0.24 mM N^6, 2′-*O*-dibutyryladenosine 3′:5′-cyclic monophosphate, (dbcAMP; Sigma-Aldrich). cRNAs (40 ng/μl) and 4 mM MSK1 morpholino oligonucleotide (MO; CCTCCCCCTCCATCTTCACCCTCTT, Gene Tools,

Philomath, OR) were microinjected into the oocytes using a Femtojet constant flow system (Eppendorf, Hamburg, Germany). The oocytes were cultured in TYH medium (Toyoda et al., 1971) containing bovine serum albumin (BSA; 4 mg/ml).

Immunoblot analysis

Proteins were separated by SDS-PAGE and transferred onto Immobilon-P polyvinylidene difluoride membranes (Millipore, Bedford, MA). The blots were blocked with 20 mM Tris/HCl, pH 7.5, containing 5% skim milk or BSA, 0.1% Tween-20, and 0.15 M NaCl, incubated with primary antibodies, and then treated with secondary antibodies conjugated with horseradish peroxidase. The immunoreactive proteins were visualized by using an ECL detection system (GE Healthcare, Piscataway, NJ).

Immunostaining analysis

Mouse ovarian and oviductal tissues were fixed in 4% paraformaldehyde at 4 °C overnight, embedded in paraffin, and sliced into 5-μm sections. The sections were treated with 10 mM Tris/HCl, pH 8.0, containing 1 μg/ml proteinase K, and 1 mM EDTA at 37 °C for 30 min, boiled in 10 mM trisodium citrate dihydrate and 10 mM citric acid monohydrate for 5 min, and then treated with phosphate buffered saline, PBS, containing 1% Triton X-100 at 4 °C for 20 min. The sections were blocked with PBS containing 3% goat serum and 0.05%

Tween-20 at room temperature for 60 min, incubated with primary antibodies, reacted with secondary antibodies conjugated with Alexa Fluor 488 or 568 at room temperature for 60 min, counterstained with Hoechst 33342, and then viewed under an IX71 fluorescence microscope (Olympus, Tokyo, Japan), as described previously (Kimura et al., 2009).

RNA synthesis in vitro

RNAs were synthesized by T7 polymerase using a RiboMAX large scale RNA production system-T7 kit (Promega, Madison, WI). The RNAs were treated with RQ1 RNase-free DNase (Promega) at 37 °C for 20 min, extracted with phenol/chloroform, precipitated with ethanol, dissolved in 10 mM Tris/HCl, pH 7.4, containing 0.1 mM EDTA, applied to MicroSpin G-25 columns (GE Healthcare), and stored at −80 °C.

Cell culture and immunoprecipitation

HEK293T cells were cultured in Dulbecco's modified Eagle's medium (Wako) supplemented with 10% fetal bovine serum, 100 U/ml penicillin, and 0.1 mg/ml streptomycin at 37 °C under 5% CO^2 in air. Cells were transfected with expression plasmid encoding FLAG–HA-tagged MSK1 using a PerFectin transfection reagent (Genlantis, San Diego, CA). After 48-h incubation, cells were cultured in serum-free medium for 24 h, and then treated with 1 μM TPA, 12-*O*-tetradecanoylphorbol 13-acetate (LC Laboratories, Woburn, MA) for 60

min. Cells were lysed with 25 mM Tris/HCl, pH 7.5, containing 0.15 M NaCl, 0.1% SDS, 1% NP-40, 1 mM EDTA, 1 μg/ml aprotinin, 1 μg/ml pepstatin, 1 μg/ml leupeptin, 50 μg/ml PMSF, 1 mM DTT, 20 mM NaF, and 0.5 mM Na_3VO_4. The cell lysates containing recombinant MSK1 were subjected to immunoprecipitation using anti-FLAG M2 agarose beads (Sigma-Aldrich). The purity of the recombinant protein was evaluated by SDS-PAGE (Fig. 1).

In vitro kinase assay

The assays were carried out in 10 mM Tris/HCl, pH 7.5, containing 10 mM $MgCl_2$, 0.1 mM DTT, 0.1 mM Na_3VO_4, 50 μM NaF, 10 μM ATP, and 2.5 μCi [γ-^{32}P]ATP (MP Biomedicals, Santa Ana, CA). GST-tagged proteins (1 μg) were incubated with MSK1 (0.1 μg) purified from HEK293T cells in the above buffer at 30 °C for 15 min, and subjected to SDS-PAGE. Proteins were visualized by Coomassie briliant blue (CBB) staining and autoradiography.

Statistical analysis

Data are presented as mean values ± S.E. (n = 3). The Student's t-test was used for statistical analysis; significance was assumed for $p<0.05$.

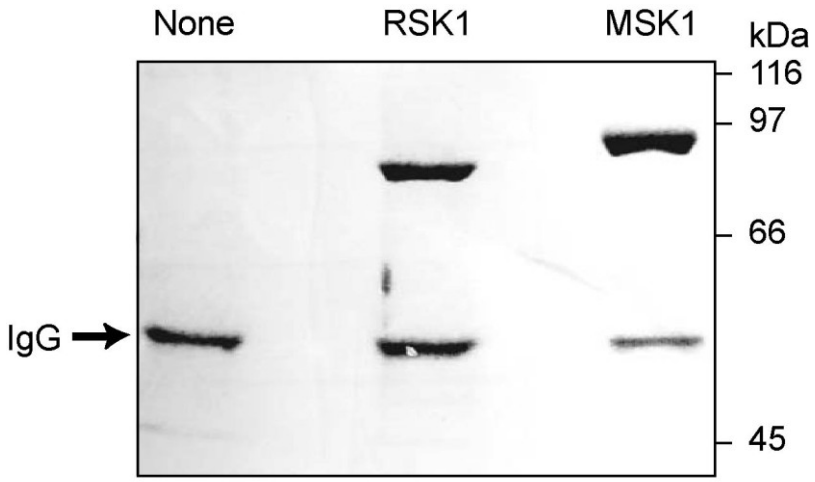

Fig. 1. Purification of MSK1 and RSK1 from HEK293T cells. HEK293T cells were transfected with expression plasmids, pcDNA3/FLAG-HA/MSK1. Cells were cultured in Dulbecco's modified Eagle's medium supplemented with 10% fetal bovine serum, 100 U/ml penicillin, and 0.1 mg/ml streptomycin at 37 ºC for 48 h under 5% CO_2 in air, incubated in the serum-free medium for 24 h, and then treated with 1 μM TPA for 60 min. The cell lysates were subjected to immunoprecipitaiton using anti-FLAG M2 agarose beads. Proteins in the immunoprecipitate were separated by SDS-PAGE and stained with CBB. As a control, cells were transfected with only pcDNA3/FLAG-HA vector (None).

RESULTS

Expression of Msk1 and Msk2 in mouse oocytes

Ubiquitous expression of *Msk1* and *Msk2* has been reported in mouse tissues (Deak et al., 1998). I initially carried out RT-PCR to examine expression of these two genes in the mouse oocytes (Fig. 2A). *Msk1* was expressed in the oocytes at the GV stage, and the metaphase II-stage oocytes still contained *Msk1* mRNA. No *Msk2* expression was found in the oocytes at both stages. As expected, immunoblot analysis indicated the presence of MSK1 in the GV- and metaphase-II oocytes (Fig. 2B). Activation of human MSK1 requires phosphorylation by ERK1/2 at S360, T581 and T700 (S359, T645 and T824 in mouse MSK1, respectively) in somatic cells (Brami-Cherrier et al., 2009). In this study, I used anti-phosphorylated MSK1 antibody that recognized phosphorylated T581 and T645 of human and mouse MSK1, respectively. Interestingly, the phosphorylated form of MSK1 was found only in the metaphase-II oocytes (Fig. 2B). These data suggest that the mouse oocytes contain MSK1 that is activated by phosphorylation after the GV stage during oocyte maturation.

Subcellular localization of phosphorylated MSK1

When immunostaining analysis of ovarian and oviductal sections was carried out, MSK1 was widely distributed in granulosa and cumulus cells and

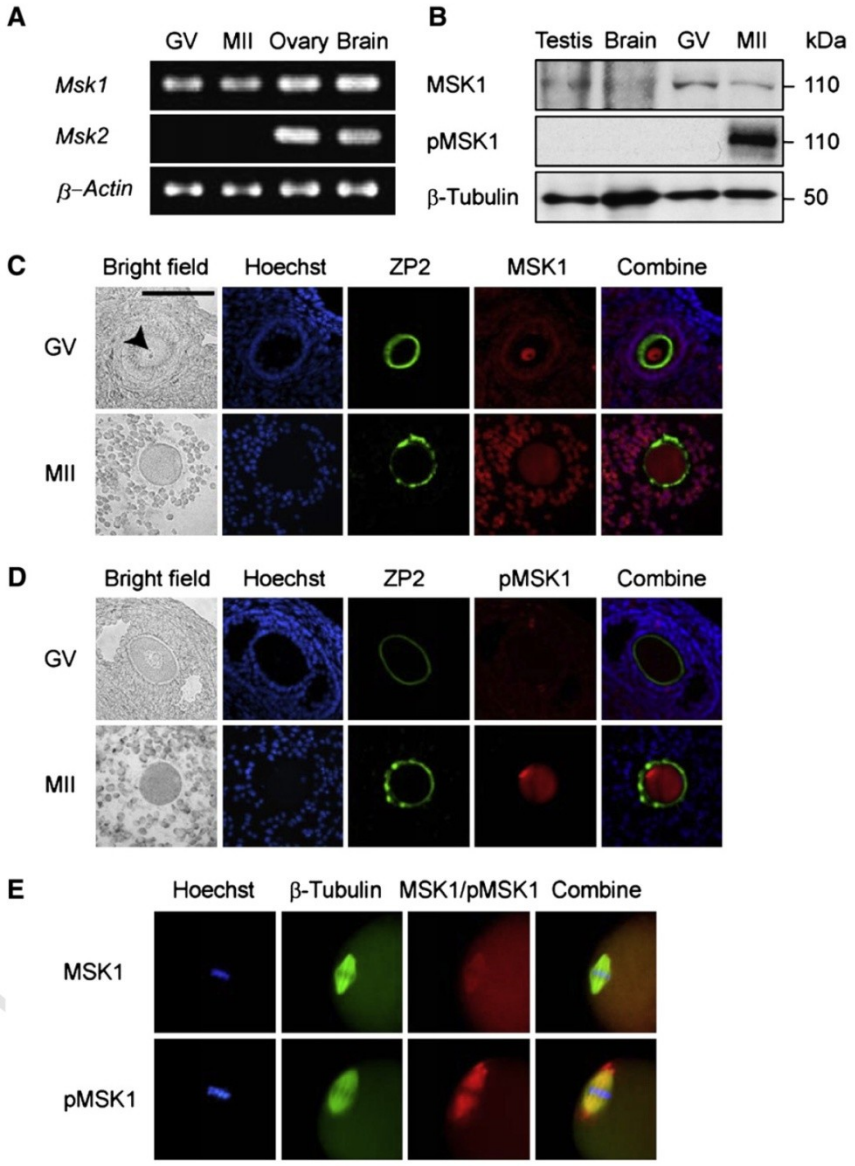

Fig. 2. Expression and localization of mouse MSK1 and MSK2. (A) RT-PCR analysis. Total RNAs were prepared from the GV- and metaphase II (MII)-stage oocytes, ovary, and brain of mice, and subjected to RT-PCR. (B) Immunoblot analysis. Whole protein extracts of GV- and MII-stage oocytes (50 cells/lane) were analyzed using anti-MSK1, anti-phosphorylated MSK1 (pMSK1), and β-tubulin. Mouse testicular and brain extracts (4 μg/lane) were also analyzed. (C) Immunostaining analysis. Mouse ovarian and oviductal sections containing the GV- and MII-stage oocytes, respectively, were probed by using anti-ZP2 (green) and anti-MSK1 (red) antibodies, and counterstained with Hoechst 33342 (blue). An arrow indicates the GV. Scale bar = 100 μm. (D) Presence of pMSK1 in the MII oocytes. Sections were probed by using anti-ZP2 (green) and anti-pMSK1 antibodies (red), and counterstained with Hoechst 33342. Note that pMSK1 is present only in the MII oocytes. (E) Localization of pMSK1 in the bipolar spindle. The MII oocytes were stained with anti-β-tubulin (green) and anti-MSK1 or anti-pMSK1 (red) antibodies, and counterstained with Hoechst 33342.

the oocytes at the GV and metaphase-II stages (Fig. 2C). In the GV and metaphase-II oocytes, MSK1 was predominantly present in the GV and cytoplasm, respectively. No significant signal of phosphorylated MSK1 was found in the GV-stage oocytes, and granulosa and cumulus cells (Fig. 2D). Importantly, phosphorylated MSK1was distributed throughout the cytoplasm of the metaphase II-stage oocytes, and was noticeably enriched within the metaphase-II plate. As compared with unphosphorylated MSK1, phosphorylated MSK1 was abundantly co-localized with β-tubulin in the bipolar metaphase-II spindle (Fig. 2E). Thus, phosphorylated MSK1 may function in bipolar spindle formation.

Phosphorylation of MSK1 through Mos–MAPK pathway

I next examined whether phosphorylation of MSK1 in the metaphase-II oocytes is dependent on the Mos–MAPK pathway. The GV-stage oocytes underwent spontaneous maturation for 24 h in the presence of U0126, a potent inhibitor specific for MEK1/2 located immediately upstream of ERK1/2 in the Mos–MAPK pathway (Yu et al., 2007). Approximately 70% of total oocytes resumed the meiotic cell cycle in the absence of the inhibitor, and were arrested at the metaphase-II stage (Fig. 3A). In the presence of U0126, most oocytes (71%) were maintained at the GV stage, and no metaphase-II oocyte was found. As described previously (Tong et al., 2003), approximately 14% of the oocytes extruded large polar bodies and formed no spindles (Fig. 3A and B). Moreover, the abnormal oocytes containing large polar bodies possessed no phosphorylated

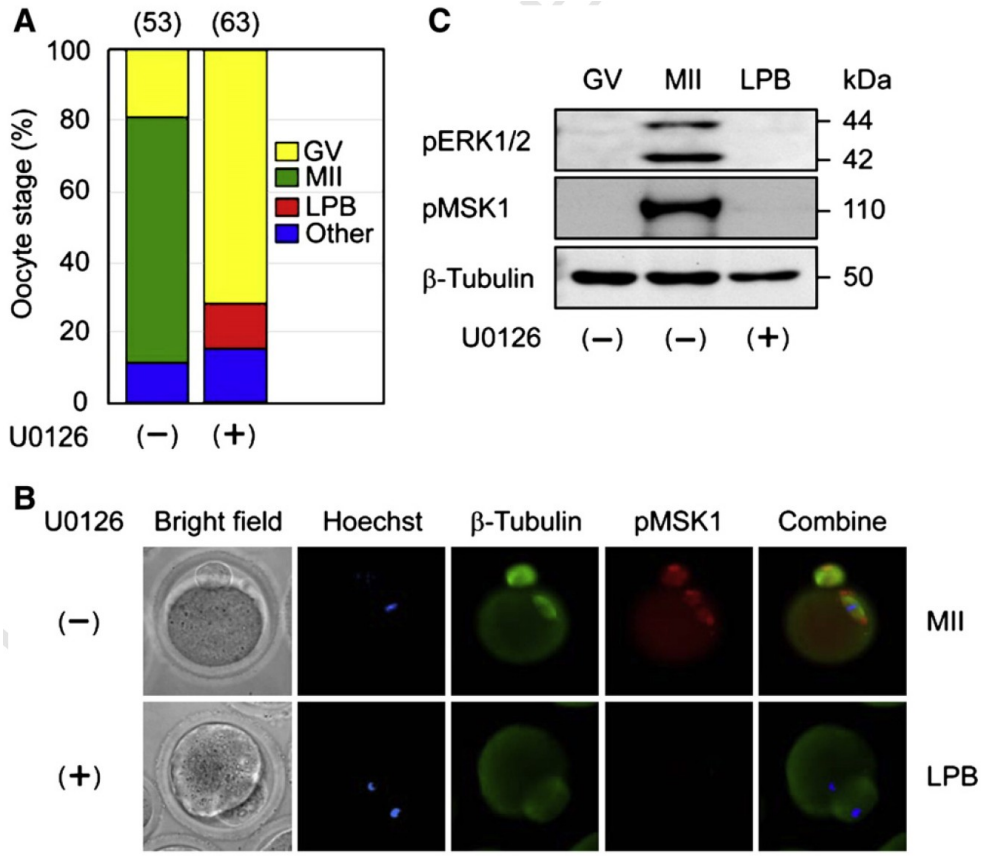

Fig. 3. Phosphorylation of MSK1 through Mos–MAPK pathway. (A) Effect of U0126 on oocyte maturation. The GV-stage oocytes were cultured for 24 h with (+) or without (−) a MEK1/2-specific inhibitor, U0126 (0.1 mM). After incubation, the ratio of oocytes at the GV, metaphase-II (MII), large polar body (LPB), and other stages was counted. Numbers in parentheses indicate those of the oocytes examined. (B) Immunostaining analysis. The GV-stage oocytes were cultured in the absence (−) or presence (+) of 0.1 mM U0126 for 24 h, and stained with anti-β-tubulin (green) and anti-phosphorylated MSK1 (pMSK1, red) antibodies, and Hoechst 33342 (blue). (C) Immunoblot analysis. The LPB oocytes were prepared by incubation of the GV-stage oocytes in the presence (+) of 60 μM U0126 for 24 h. The oocytes at the GV and MII stages were directly subjected to immunoblot analysis. Proteins (50 oocytes/lane) were analyzed using anti-phosphorylated ERK1/2 (pERK1/2), anti-pMSK1, and anti-β-tubulin antibodies.

forms of ERK1/2 and MSK1 (Fig. 3C). These results suggest that MSK1 is phosphorylated by the Mos–MAPK pathway during oocyte maturation.

Involvement of MSK1 in metaphase-II arrest

To clarify the role of MSK1 in the metaphase-II arrest further, I microinjected an *Msk1* MO into the oocytes at the GV stage, which were incubated for 12 h in the presence of dbcAMP and then matured for 24 h in the absence of dbcAMP (Fig. 4). The *Msk1* MO only partially (approximately 40%) prevented the accumulation of MSK1 protein in the metaphase II-stage oocytes, and failed to affect the metaphase-II arrest. I also examined effects of two chemical inhibitors, H89 and Ro31-8220 on release from the metaphase-II arrest (Fig. 5). Although H89 and Ro31-8220 are commonly used to inhibit the activities of PKA and PKC, respectively, these two chemicals are also known to interfere with the MSK1 activity (Espino et al., 2006; Kawaguchi et al., 2009). When the metaphase-II oocytes were incubated with or without H89 for 6 h, the metaphase-II arrest was 15 and 93% released by the presence of 30 and 60 μM H89, respectively (Fig. 5A). In the case of 5 μM Ro31-8220, the oocytes were 97% released from the metaphase-II arrest (Fig. 5B). I observed chromosome segregation and abnormal pronuclear formation 2 and 4 h after addition of 60 μM H89, respectively (Fig. 5C). In the H89-treated oocytes, phosphorylated MSK1 was spread throughout the cytoplasm, owing to the loss of bipolar metaphase-II spindle (Fig. 6). Moreover, immunoblot analysis revealed that cyclin B1 is dramatically degraded 2 h after incubation in the presence of 60 μM

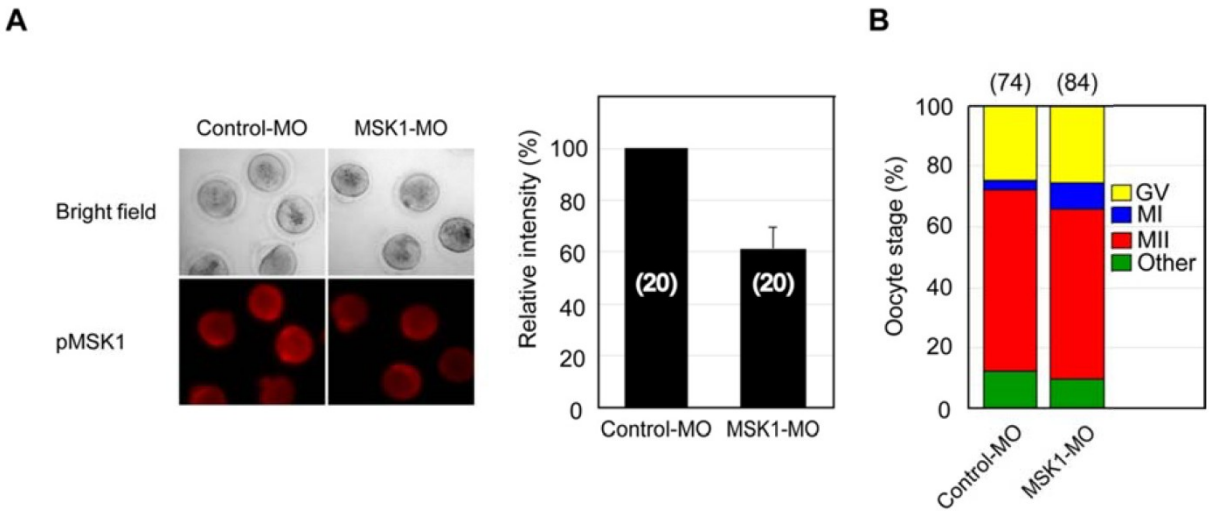

Fig. 4. *Msk1* knockdown by morpholino oligonucleotide (MO) injection. (A) Microinjection of *Msk1* MO. Mouse oocytes at the germinal vesicle (GV) stage were microinjected with 4 mM *Msk1* MO or negative control MO using a Femtojet constant flow system, treated with dbcAMP for 12 h, incubated in the absence of dbcAMP for 24 h, and then stained with anti-phosphorylated MSK1 (pMSK1, red) antibody. Fluorescence intensities of the whole oocytes were measured. Data are presented as mean values ± S.E. (n = 3; p = 0.06). (B) Ratio of *Msk1* MO-injected oocytes. After incubation, the oocytes at the GV, metaphase-I (MI), metaphase-II (MII), and other stages were counted. Numbers in parentheses indicate those of the oocytes examined.

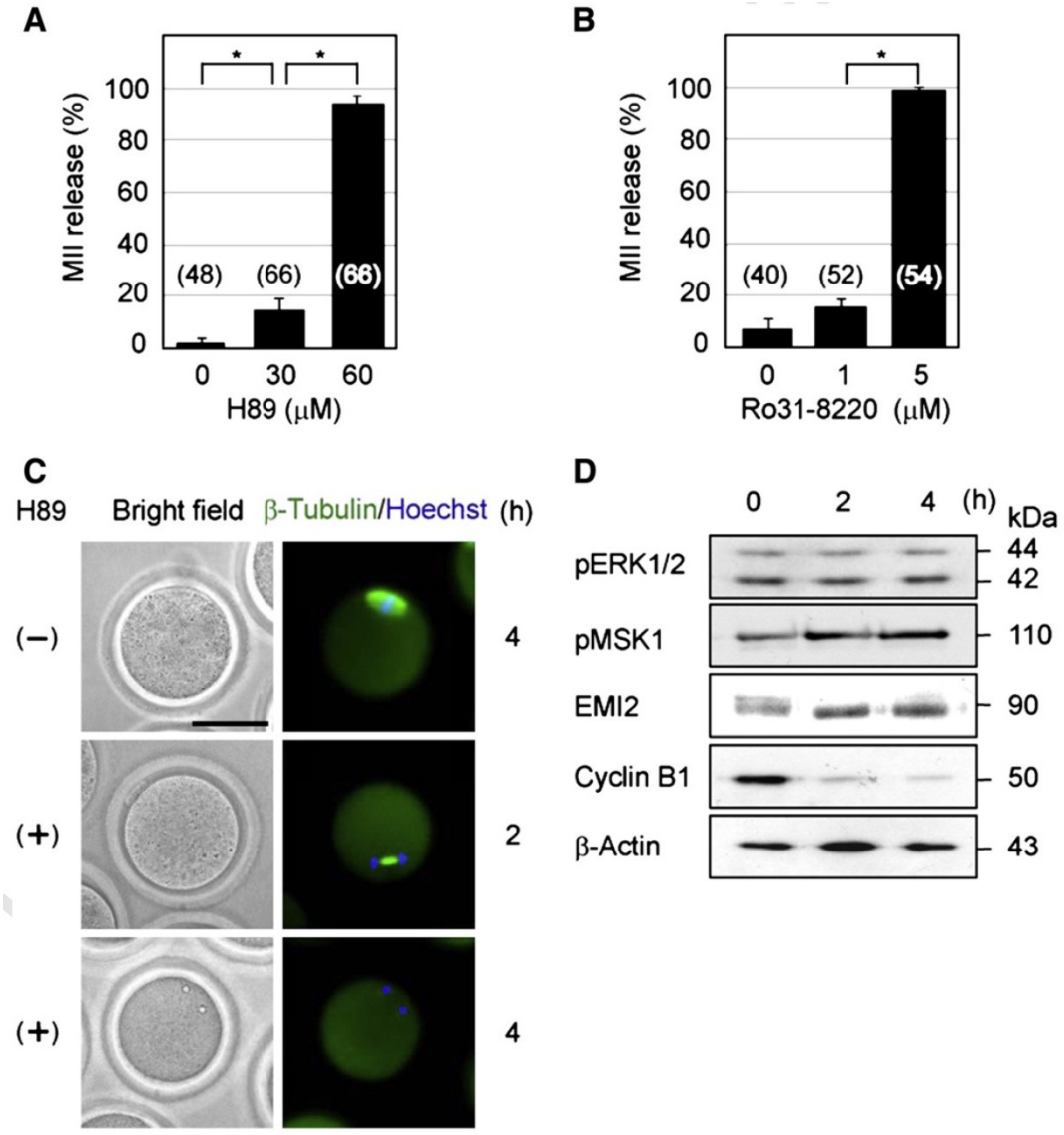

Fig. 5. Involvement of MSK1 in the metaphase-II arrest. (A) Release from the metaphase-II (MII) arrest by H89. The MII oocytes were incubated with or without MSK1 inhibitor H89 (0, 30, and 60 μM) for 6 h. The numbers in parentheses indicate those of the MII oocytes examined. *$p<0.05$. (B) Release from the MII arrest by Ro31-8220. The MII oocytes were incubated with or without MSK inhibitor Ro31-8220 (0, 1, and 5 μM). (C) Immunostaining analysis. The MII oocytes were incubated in the presence of H89 (60 μM) for 2 and 4 h, and then stained with Hoechst 33342 (blue) and anti-β-tubulin antibody (green). Scale bar = 50 μm. (D) Immunoblot analysis. The MII oocytes were incubated in the presence of H89 (60 μM) for 0, 2, and 4 h, and proteins (30 oocytes/lane) were analyzed using antibodies against phosphorylated ERK1/2 (pERK1/2), anti-phosphorylated MSK1 (pMSK1), EMI2, cyclin B1, and β-actin.

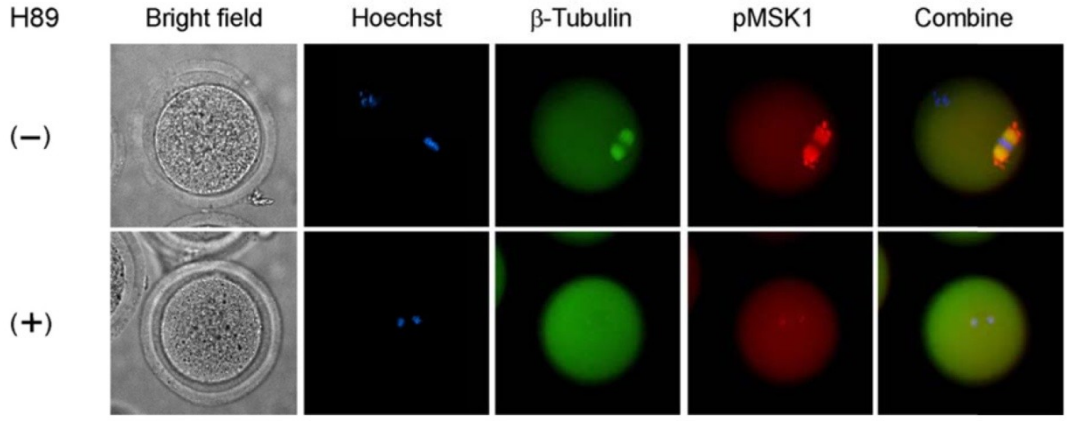

Fig. 6. Immunostaining of the metaphase-II oocytes treated with H89. The metaphase-II oocytes were incubated in the absence (-) or presence (+) of 60 μM H89 for 4 h, and stained with anti-β-tubulin (green) and anti-phosphorylated MSK1 (pMSK1, red) antibodies, and with Hoechst 33342 (blue).

H89 (Fig. 5D). The levels of phosphorylated ERK1/2, phosphorylated MSK1, and EMI2 remained relatively constant throughout incubation. These results suggest that the inhibition of the kinase activity of phosphorylated MSK1 by H89 may result in the failure of EMI2 phosphorylation/activation, leading to the degradation of cyclin B1.

Phosphorylation of EMI2 by MSK1

To ascertain the possibility that MSK1 directly phosphorylates EMI2 to maintain the metaphase-II arrest, I carried out kinase assays in vitro using GST-fused proteins (Fig. 7). In *Xenopus*, four Ser/Thr residues of Emi2 at positions S335, T336, S342, and S344 are phosphorylated by RSKs (Inoue et al., 2007; Nishiyama et al., 2007). This phosphorylation is required for up-regulation of the stability and activity of Emi2 in the oocytes. Since these four residues of *Xenopus* Emi2 are conserved in the mouse, human, and zebrafish counterparts (Fig. 7A), it is assumed that mouse MSK1 as well as *Xenopus* RSKs is capable of phosphorylating the same Ser/Thr residues of EMI2. I thus prepared phosphorylated MSK1 from HEK293T cells that had been cultured with TPA (Figs. 1 and 8), and then carried out in vitro kinase assays using the purified protein. Both EMI2 and transcription factor CREB (Deak et al., 1998) as a positive control were efficiently phosphorylated by MSK1 (Fig. 7B). Phosphorylation of EMI2 by MSK1 was 34 and 87% inhibited by addition

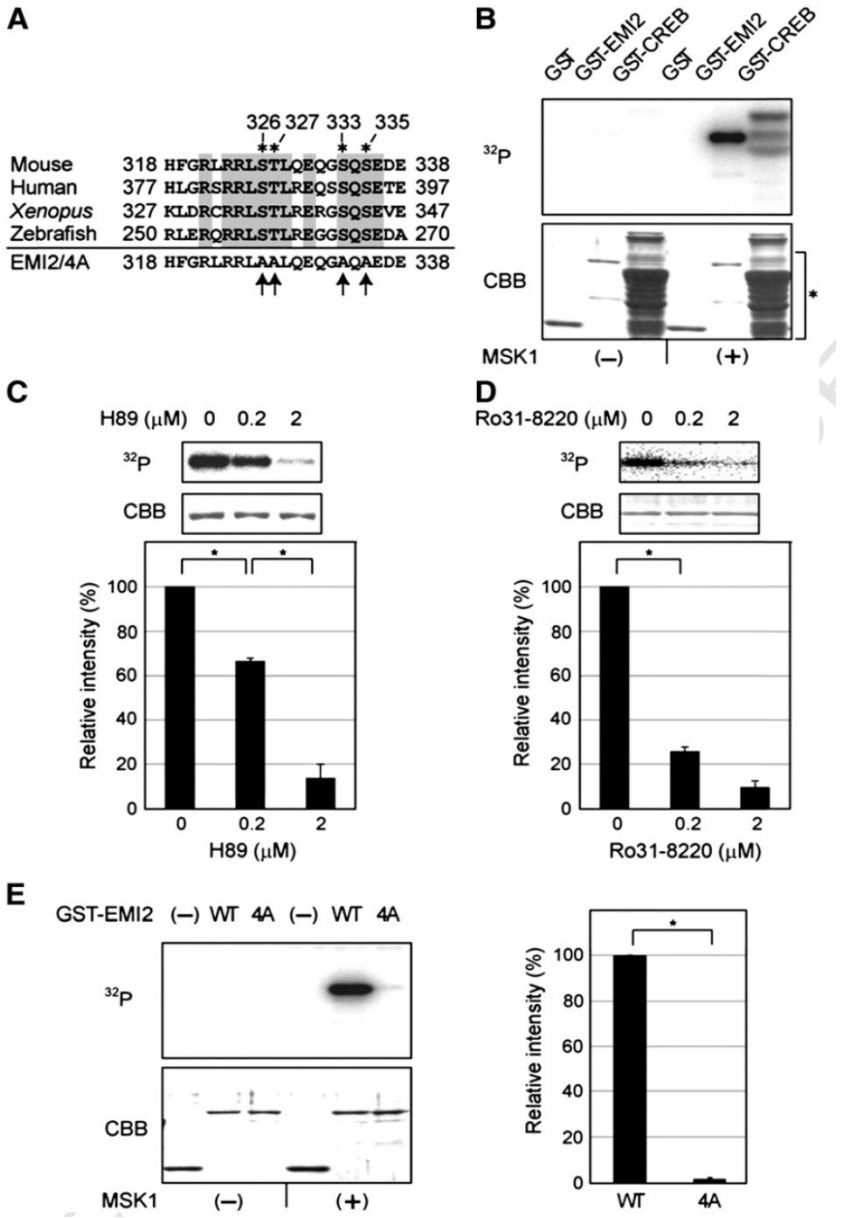

Fig. 7. Phosphorylation of EMI2 by MSK1. (A) Alignment of the amino acid sequences of EMI2 among mouse, human, *Xenopus,* and zebrafish. Gray boxes and asterisks indicate the conserved residues and possible phosphorylation sites by *Xenopus* RSKs, respectively. The sequence of an EMI2/4A mutant is also aligned. (B) In vitro kinase assay. GST-tagged EMI2 (1 μg) was incubated with (+) or without (−) purified MSK1 (0.1 μg) in the presence of [γ-^{32}P]ATP, separated by SDS-PAGE, and analyzed by autoradiography and CBB staining. GST alone and GST-tagged CREB were used as negative and positive controls, respectively. An asterisk indicates background proteins. (C and D) Inhibition of MSK1 kinase activity. Purified MSK1 was incubated with GST-tagged EMI2 in the absence and presence (0, 0.2, and 2 μM each) of H89 (C) or of Ro31-8220 (D). *$p<0.05$. (E) Phosphorylation of EMI2/4A by MSK1. Wild-type (WT) EMI2 and EMI2/4A were incubated with (+) or without (−) MSK1. *$p<0.05$.

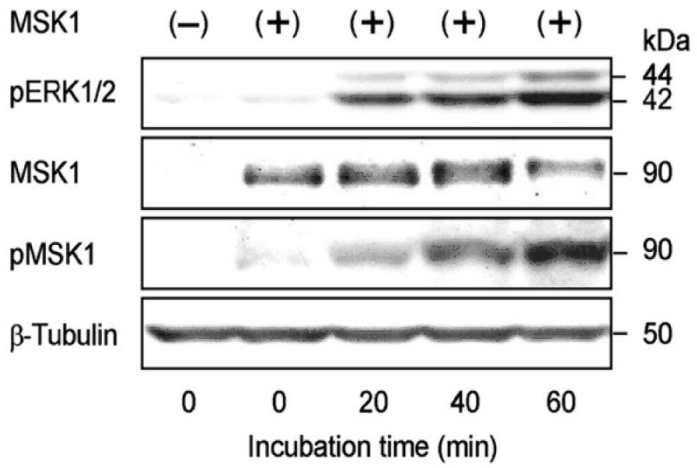

Fig. 8. Up-regulation of the MSK1 activity by TPA. Immunoblot analysis of TPA-treated cell lysates. HEK293T cells were transfected with pcDNA3/FLAG-HA only (-) or pcDNA3/FLAG-HA/MSK1 (+), as described in Fig. 1, and then treated without (0 min) or with 1 μM TPA for 20, 40, and 60 min. Proteins in of cell lysates were analyzed by immunoblotting using antibody against phosphorylated ERK1/2 (pERK1/2), MSK1, phosphorylated MSK1 (pMSK1), or β-tubulin.

of 0.2 and 2 μM H89 (74 and 87% for 0.2 and 2 μM Ro31-8220), respectively (Fig. 7C and D). I further examined whether MSK1 phosphorylates four Ser/Thr residues of EMI2 at S326, T327, S333, and S335 (Fig. 7E). A GST-tagged EMI2 mutant protein, termed EMI2/4A, in which these four Ser/Thr residues were all substituted with Ala (Fig. 7A), was analyzed by in vitro kinase assays. The EMI2/4A mutant was barely phosphorylated by MSK1 as compared to wild-type EMI2 (Fig. 7E). Thus, MSK1 possesses the ability to phosphorylate S326, T327, S333, and S335 on the EMI2 molecule.

Up-regulation of EMI2 activity by S326, T327, S333, and S335 phosphorylation

Ala substitutions of S335 and T336 or T336, S342, and S344 in *Xenopus* Emi2 have been demonstrated to result in protein degradation dependent of E3 ubiquitin ligase SCF β-TrCP during oocyte maturation (Inoue et al., 2007; Nishiyama et al., 2007). SCF β-TrCP recognizes the phosphodegron sequence, Asp-Ser-Ala-Phe-His-Ser, of *Xenopus* Emi2 at residues 283–313. Because the *Xenopus* phosphodegron sequence is conserved in the mouse EMI2 sequence, Asp-Ser-Gly-Phe-Cys-Ser, at residues 274–279, I constructed expression plasmids encoding an EMI2/DSG mutant carrying Ala substitutions at S275 and S279, and an EMI2/DSG/4A mutant. To examine the inhibitory activities of these two EMI2 mutants toward APC/C in an experimental model system (Suzuki et al., 2010), I microinjected synthetic RNA encoding HA-tagged EMI2/DSG or EMI2/DSG/4A mutant into the GV-stage oocytes containing a negligibly small amount of endogenous EMI2 (Madgwick et al., 2006; Shoji et

al., 2006). The RNA-injected oocytes were cultured in the presence of dbcAMP for 2 h, and then underwent spontaneous maturation in the absence of dbcAMP for 20 h (Fig. 9A). Exogenously expressed EMI2 is known to induce the metaphase-I arrest under these conditions (Suzuki et al., 2010). Immunostaining analysis using anti-HA antibody verified production of EMI2/DSG and EMI2/DSG/4A mutant proteins in the oocytes after the 20-h incubation (Fig. 9B). Importantly, the oocytes containing the EMI2/DSG protein were mostly (84%) arrested at the metaphase-I stage, whereas a significantly low level (43%) of the metaphase-I arrest was found in the oocytes containing the EMI2/DSG/4A protein (Fig. 9C). In contrast, 40% of total EMI2/DSG/4A-containing oocytes underwent meiotic maturation and progressed to the metaphase-II stage. Since endogenously produced MSK1 was phosphorylated in the EMI2/DSG-containing oocytes arrested at the metaphase-I stage (Fig. 10), the phosphorylation of EMI2 at S326, T327, S333, and S335 is probably required for the metaphase-I arrest of the oocytes. Thus, MSK1 may be involved in the metaphase-II arrest through phosphorylation of EMI2 in the mouse. On the basis of the data obtained, I propose a schematic model for the metaphase-II arrest in the mouse oocyte (Fig. 9D).

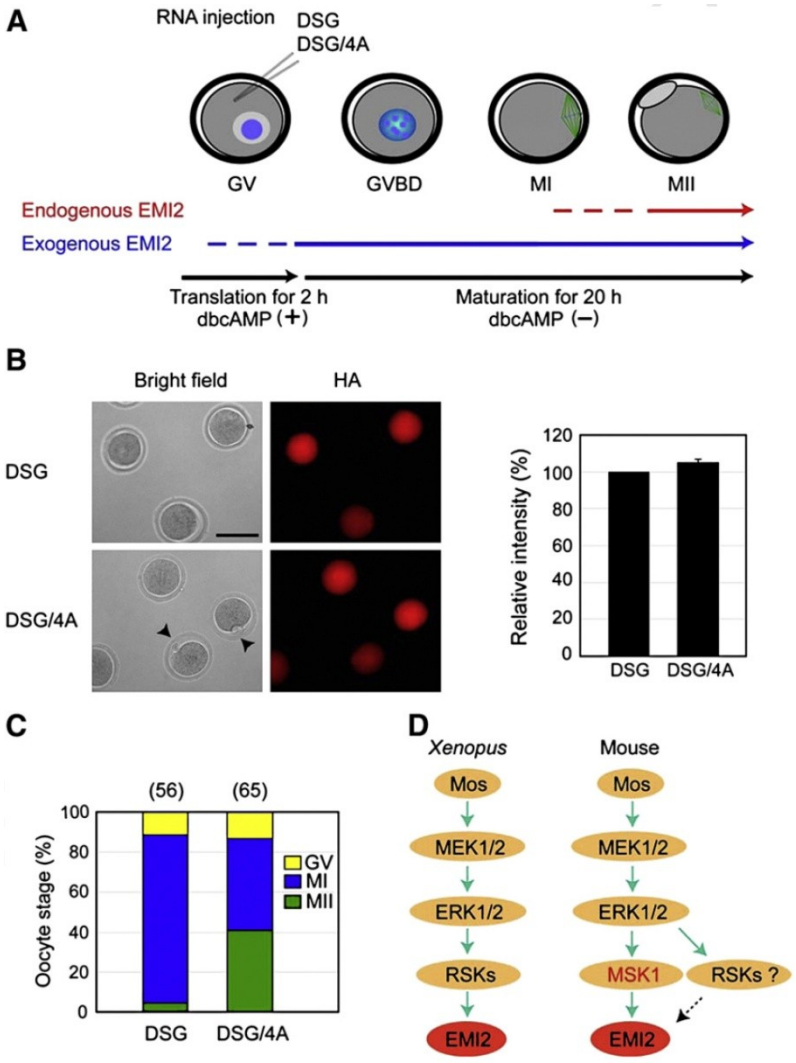

Fig. 9. EMI2 activity is up-regulated by phosphorylation at S326, T327, S333 and S335. (A) Experimental protocol for expression of EMI2/DSG and EMI/DSG/4A mutants. The GV-stage oocytes were microinjected with polyadenylated RNA encoding HA-tagged EMI2/DSG and EMI2/DSG/4A (termed DSG and DSG/4A, respectively), and incubated in the presence of dbcAMP for 2 h. After incubation in the absence of dbcAMP for 20 h, the oocytes at different maturation stages were counted. MI, metaphase I; MII, metaphase II. Note that the oocytes contain a negligibly small amount of endogenous EMI2 until the MI/MII transition. (B) Immunostaining analysis. The oocytes were immunostained with anti-HA antibody (red). Fluorescence intensities of the oocytes expressing HA-tagged DSG or DSG/4A (15 cells each) were measured. Arrows indicate polar bodies. Scale bar = 100 μm. (C) Ratio of oocytes at GV, MI, and MII stages. Numbers in parentheses indicate those of the oocytes examined. (D) Schematic model for the MII arrest in the mouse oocytes. RSKs regulate the Emi2 activity in the *Xenopus* oocytes. In the mouse oocytes, the EMI2 activity may be regulated predominantly by MSK1, although participation of RSKs cannot be neglected completely.

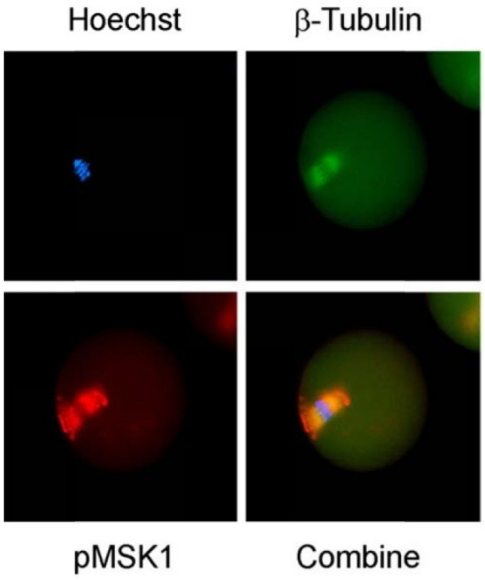

Fig. 10. Phosphorylation of MSK1 in metaphase-I arrested oocytes. The germinal vesicle-stage oocytes were microinjected with polyadenylated RNA encoding HA-tagged EMI2/DSG, and incubated in the presence of dbcAMP for 2 h. After incubation in the absence of dbcAMP for 20 h, the oocytes were stained with anti-β-tubulin (green) and anti-phosphorylated MSK1 (pMSK1, red) antibodies, and counterstained with Hoechst 33342 (blue).

DISCUSSION

This study describes the subcellular localization and possible role of MSK1 in the metaphase-II arrest of the mouse oocyte. Two MSKs, MSK1 and MSK2, are ubiquitously expressed and predominantly localized in the cell nucleus (Deak et al., 1998). Of these two MSKs, only MSK1 is present in the GV and cytoplasm of oocytes at the GV and metaphase-II stages, respectively (Fig. 2). MSK1 is changed to the active form by Ser/Thr phosphorylation after the GV stage, and the phosphorylated protein is enriched in the bipolar spindle in the metaphase-I/II oocytes (Figs. 2 and 10). In addition, phosphorylated MSK1 is capable of phosphorylating four Ser/Thr residues of EMI2 (Fig. 7), which is required for the CSF arrest (Fig. 9). These findings suggest that MSK1 may play a key role in the metaphase-II arrest of oocytes through phosphorylation of EMI2 in the mouse. It is important to note that consistent with previous data regarding the localization of ERK1/2 (Fan et al., 2009; Sasseville et al., 2010), MSK1 is also localized in granulosa and cumulus cells (Fig. 2). This observation implies a functional role of MSK1 in these cells.

Phosphorylated MSK1 is abundantly present in the bipolar spindle of metaphase-I/II oocytes (Figs. 2 and 10), as described above. ERK1/2 are thought to phosphorylate MSK1 as a target protein in somatic cells (Deak et al., 1998). In the mouse oocytes, phosphorylation of ERK1/2 is directly catalyzed by MEK1/2 that are activated by Mos (Verlhac et al., 1996), as shown in Fig. 9D. Indeed, both the inhibition of ERK1/2 activation by the MEK inhibitor U0126 (Tong et al., 2003) and the deletion of Mos (Colledge et al., 1994; Hashimoto et

al., 1994) have been reported to induce to release the metaphase-II arrest. Since ERK1/2 are activated by MEK1/2 immediately after GV breakdown in the mouse oocytes (Tsurumi et al., 2004), activation of MSK1 probably takes place successively through phosphorylation by ERK1/2 (Fig. 3). Phosphorylated MSK1 may then act on activation of EMI2 present in the bipolar spindle (Suzuki et al., 2010). It is also suggested that phosphorylated MSK1 may function in phosphorylation of unknown target protein(s) localized in the oocyte spindle. Indeed, the loss of active ERK1/2 has been reported to result in the abnormal shape of bipolar spindle, because of no activation of the ERK1/2 substrates, including MISS and DOC1R (Lefebvre et al., 2002; Terret et al., 2003).

MO is conventionally utilized to inhibit production of target proteins in the mouse oocytes; however, accumulation of some proteins present in the GV-stage oocytes is not entirely prevented by MO (Chang et al., 2009; Yuan et al., 2010). In the present study, despite injection of *Msk1* MO into the GV-stage oocytes, the *Msk1* knockdown oocytes still contained a relatively large amount of MSK1 after meiotic resumption, and failed to affect the meiotic arrest at the metaphase-II stage (Fig. 4). This phenotype may be due to the possibility that MSK1 accumulation in the GV-stage oocytes is abundant enough for progression to the metaphase-II stage.

H89 acts as inhibitors of PKA and MSK1, whereas the activities of MSK1, RSKs, and PKC are predominantly inhibited by Ro31-8220 (Davies et al., 2000; Oh et al., 2010). PKA is thought to participate in meiotic arrest only at the prophase of meiosis I in the vertebrate oocytes (Perry and Verlhac, 2008). In this study, the abovementioned two inhibitors, H89 and Ro31-8220, induce to

release the metaphase-II arrest (Fig. 5). My data imply that at least MSK1 is involved in the metaphase-II arrest of mouse oocytes. This possibility appears to be supported by the fact that the RSK1/RSK2/RSK3 triple- and MSK1/MSK2 double-knockout mice both display no overt phenotype (Dumont et al., 2005; Wiggin et al., 2002). Thus, I speculate that MSK1 and RSKs may serve as a compensatory mechanism to activate/phosphorylate EMI2 in the mouse oocytes (Fig. 9D).

Both MSKs and RSKs are known to phosphorylate Ser/Thr residues in the conserved R/KXRXXS, RRXS, and RKS motifs (Hauge and Frodin, 2006). In some experiments, I examined whether mouse RSK1 possesses the ability to phosphorylate EMI2 (Fig. 11). My data demonstrated that MSK1 and RSK1 are both capable of directly phosphorylating S326, T327, S333, and S335 of mouse EMI2 (Figs. 7 and 11). When an EMI2/2A mutant carrying Ala substitutions at S326 and T327 was analyzed by in vitro kinase assays, MSK1 phosphorylated the Ser residues at positions 333 and 335 (Fig. 12). Since MSK1 fails to phosphorylate EMI2/4A mutant (Fig. 7E), either one or both of S333 and S335, in addition to S326 and T327, in the EMI2 molecule may be phosphorylated by MSK1. It is intriguing that the amino acid sequences carrying S333 and S335 contain no consensus motifs of phosphorylation sites by MSKs. Thus, further experiments are required to elucidate the detailed mechanism on MSK1-catalyzed phosphorylation of EMI2.

Since initial characterization of CSF (Masui and Markert, 1971), progress has been made in understanding the role of CSF in the oocytes at the molecular level. Recently, *Xenopus* Emi2 has been reported to be indispensable for the

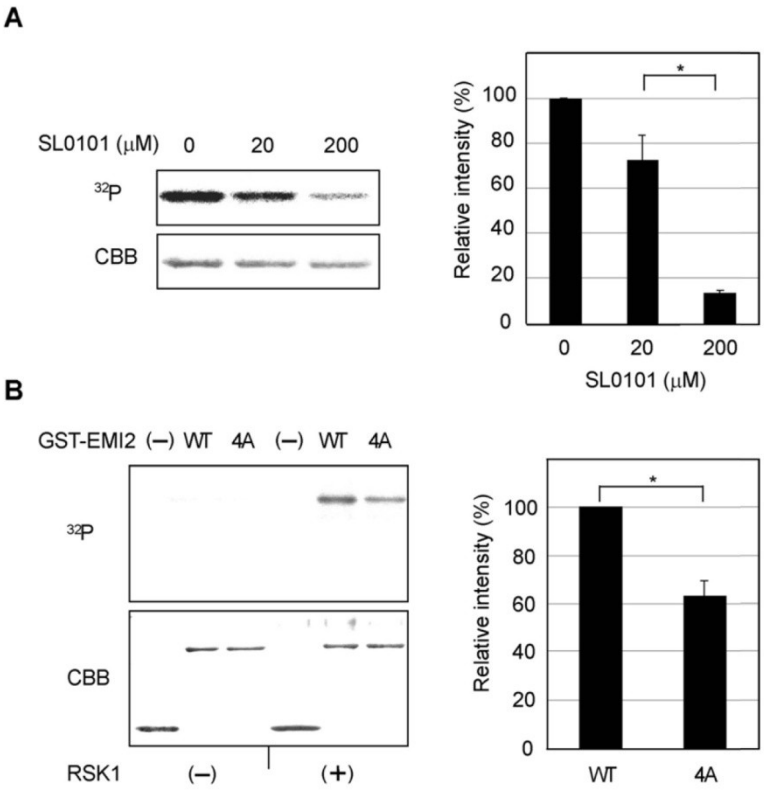

Fig. 11. Phosphorylation of EMI2 by RSK1. (A) In vitro kinase assays for phosphorylation of EMI2 by RSK1. GST-tagged EMI2 (1 μg) was incubated with purified RSK1 (0.1 μg, see Fig. 1) in the absence (0 μM) and presence of an RSK1 inhibitor, SL0101 (20 and 200 μM). Proteins were separated by SDS-PAGE and visualized by autoradiography and CBB staining. Data are presented as mean values ± S.E. (n = 3; *p<0.05). (B) In vitro kinase assays for phosphorylation of EMI2/4A by RSK1. Purified RSK1 was incubated with wild-type (WT) EMI2 or EMI2/4A (4A). GST was used as a negative control (-). Data are presented as mean values ± S.E. (n = 3; *p<0.05).

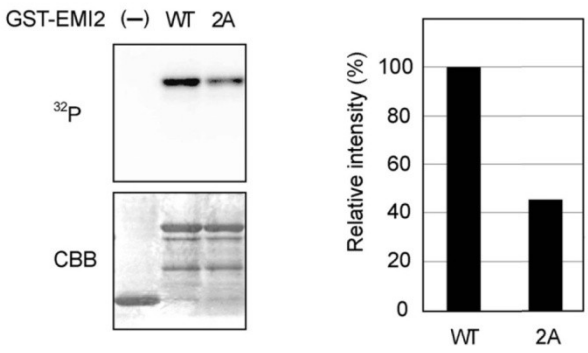

Fig. 12. Phosphorylation of EMI2/2A by MSK1. GST-tagged wild-type (WT) EMI2 and EMI2/2A (1 μg) were incubated with purified MSK1 (0.1 μg) in the presence of [γ-^{32}P]ATP, separated by SDS-PAGE, and analyzed by autoradiography and CBB staining. GST was used as a negative control (-). Data are presented as the mean values of two separate experiments.

CSF activity in the Mos–MAPK pathway (Inoue et al., 2007; Nishiyama et al., 2007); the stabilization and activation of Emi2 are promoted by its phosphorylation catalyzed by RSKs. Because RSKs are not essential for the metaphase-II arrest in the mouse oocytes (Dumont et al., 2005), it has long been believed that other kinase(s) participates in phosphorylation of EMI2. My data presented here emphasize that MSK1 is a candidate protein involved in phosphorylation of EMI2. Thus, this study proposes a novel model for direct phosphorylation of EMI2 by MSK1 in the Mos–MAPK pathway of the mouse oocyte.

CHAPTER II

p38 MAPK, in addition to the Mos-MAPK pathway, contributes to metaphase-II arrest through EMI2 phosphorylation in mouse oocytes

SUMMARY

The Mos-MAPK signaling pathway involving the Mos-MEK1/2-ERK1/2-RSK1/2/3 or MSK1-EMI2 cascade is directly linked to metaphase-II arrest of vertebrate oocytes. Another kinase downstream of Mos has been postulated to participate in the oocyte arrest, because the metaphase-II arrest is not completely released by inhibition of MEK1/2. In this study, I examined whether p38, a member of the MAPK subfamily, is regulated under the control of Mos, and contributes to the metaphase-II arrest in the mouse oocyte. Morpholino oligonucleotide-mediated depletion of Mos revealed a remarkable decrease in phosphorylation of p38. Simultaneous treatment of oocytes with two chemical inhibitors of p38 and MEK1/2 induced both release from metaphase II and degradation of cyclin B1, whereas the treatment with each of these two inhibitors had little effect. Moreover, phosphorylation of EMI2 was dramatically abolished by addition of the two inhibitors. Indeed, MNK1, a kinase downstream of p38, exhibited the ability to phosphorylate EMI2. These results suggest that in addition to the Mos-MEK1/2 pathway, the Mos-mediated p38 pathway may be implicated in the metaphase-II arrest.

INTRODUCTION

Vertebrate oocytes at the germinal-vesicle (GV) stage are arrested at prophase of meiosis I and undergo maturation after hormonal stimulation (Sagata, 1996; Kishimoto, 2003). Mature oocytes are rearrested at the metaphase of meiosis II until fertilization. The metaphase-II arrest is caused by the activity of cytostatic factor CSF (Masui and Markert, 1971) that inhibits the anaphase-promoting complex/cyclosome (APC/C), an E3 ubiquitin ligase required for degradation of cyclin B (Peters, 2006). As a consequence of cyclin B stabilization, the activity of MPF, the Cdk1-cyclin B complex (Gautier et al., 1990), is maintained at an elevated level that prevents the exit from metaphase II and parthenogenetic activation of oocytes (Yamamoto et al., 2005). In *Xenopus*, CSF-mediated arrest involves the Mos-MAPK pathway (Mos-Mek1/2-Erk1/2-Rsk1/2/3) and Emi2, a direct inhibitor of the APC/C (Sagata et al., 1989; Gross et al., 2000; Dupré et al., 2002; Schmidt et al., 2005; Tung et al., 2005). Rsks phosphorylate four Ser/Thr residues of Emi2 at positions S335, T336, S342 and S344 (Inoue et al., 2007; Nishiyama et al., 2007). Multiple phosphorylation of Emi2 upregulates its stability and inhibitory binding to the APC/C, thereby promoting the metaphase-II arrest (Wu et al., 2007).

In mice, the oocytes lacking Mos are activated without stimulation on fertilization (Colledge et al., 1994; Hashimoto et al., 1994; Araki et al., 1996; Choi et al., 1996; Verlhac et al., 1996). The EMI2-depleted oocytes sustain a low level of cyclin B after meiosis I, which leads to the failure to enter the

metaphase II (Madgwick et al., 2006; Shoji et al., 2006). Thus, both Mos and EMI2 are essential for the metaphase-II arrest in the oocytes, but the role of the components downstream of Mos is still controversial. Inhibition of MEK1/2 synthesis by siRNA has little effect on the metaphase-II arrest (Yu et al., 2007). Injection of a constitutively active form of MEK1/2 into Mos-deficient oocytes fails to activate ERK1/2 (Verlhac et al., 2000). These findings raise the possibility that another Mos-dependent kinase also plays a key role in the metaphase-II arrest.

p38 MAPK is one of the major members of the MAPK family that negatively regulates cell-cycle progression at both G1/S and G2/M in somatic cells (Thornton and Rincon, 2009). At least five Ser/Thr kinases, MSK1, MSK2, MNK1, MK2, and MK3, have been identified as p38 substrates (Cargnello and Roux, 2011). Functional analysis of p38 in the mouse oocytes suggests that this kinase regulates spindle assembly and accurate chromosome segregation through phosphorylation of MK2 (Yuan et al., 2010; Ou et al., 2010).

In this study, I examined whether p38 is regulated under the control of Mos and contributes to the metaphase-II arrest in mouse oocytes. Depletion of Mos revealed a significant decrease in phosphorylation of p38. When the Mos-mediated MEK1/2 and p38 pathways were both blocked by specific inhibitors, the metaphase-II arrest was released. Possible role of p38 in the metaphase-II arrest is discussed.

MATERIALS AND METHODS

All animal experiments performed ethically, and experimentation was in accord with the Guide for the Care and Use of Laboratory Animals at University of Tsukuba.

Plasmids

DNA fragments encoding EMI2 (Genbank ID: NP_001074772.1) and MSK1 (Genbank ID: AAQ24165.1) were amplified by polymerase chain reaction (PCR) using a mouse ovary or testis cDNA library as a template. Following sets of oligonucleotides were used as primers: 5′-GGGCGGCCGCGGATGGACTCCTCTGCTGTC-3′ and 5′-GGCTCGAGTCAGAGGCGTTTTAAGTTCCGC-3′ for EMI2; 5′-GCCTCGAGAGGGTGAAGATGGAGGG-3′ and 5′-GCTCTAGAACATACCTCAGGCACATG-3′ for MSK1. The amplified fragments were introduced into a pcDNA3/FLAG-HA vector. To prepare a pGEX4T-1/EMI2 plasmid containing the EMI2 sequence with residues 288-383, DNA fragments were PCR-amplified using pcDNA3/FLAG-HA/EMI2 as the template, and introduced into pGEX4T-1. A pcDNA3.1-poly(A)/FLAG-HA/EMI2 plasmid was prepared by introducing the *Kpn*I/*Bam*HI fragment of pcDNA3/FLAG-HA/EMI2 into pcDNA3.1-poly(A) as previously described (Yamazaki et al., 2007). In vitro site-directed mutagenesis

was carried out according to manufacturer's protocol (Agilent Technology, Santa Clara, CA).

Antibodies

Synthetic phosphorylated peptide, Cys-Arg-Leu-Arg-Arg-Leu-phospho Ser-phospho Thr-Leu-Gln-Glu-Gln-Gly, corresponding to the 12-residues sequence of EMI2 at positions 321-332 was conjugated to maleimide-activated keyhole limpet hemocyanin (KLH) or bovine serum albumin (BSA) according to the manufacturer's protocol (Thermo Fisher Scientific, Waltham, MA). The protein KLH-conjugated peptide was emulsified with Freund's complete (Difco Laboratories, Detroit, MI) or incomplete adjuvant (Wako, Osaka, Japan), and injected into female Japanese white rabbits (Japan SLC, Shizuoka, Japan). Antibody against the unphosphorylated form of EMI2 was removed from serum using a Sepharose 4B column previously coupled with glutathione *S*-transferase (GST)-tagged EMI2 at residues 288-383. Anti-phosphorylated EMI2 antibody was purified using a Sepharose 4B column previously coupled with the BSA-conjugated 12-residue peptide. Anti-phosphorylated MNK1, anti-phosphorylated p38, and anti-phosphorylated ERK1/2 antibodies were purchased from Cell Signaling Technology (Danvers, MA), and anti-β-actin, anti-GAPDH, and fluorescein isothiocyanate (FITC)-conjugated anti-α-tubulin antibodies were from Sigma-Aldrich (Saint Louis, MO). Anti-cyclin B1, anti-HA and anti-Mos antibodies were purchased from Abcam (Cambridge, MA), Roche (Mannheim, Germany), and Santa Cruz Biotechnology (Santa Cruz, CA),

respectively. Horseradish peroxidase-conjugated antibodies against mouse, rat, or rabbit IgG were purchased from Jackson ImmunoResearch Laboratories (West Grove, PA).

Oocyte collection and microinjection

GV-stage oocytes were collected from ovaries of 6- to 9-week-old ICR mice (Japan SLC). The oocytes were placed in a drop of flushing-holding medium (FHM) containing 0.32 mM N^6, 2′-*O*-dibutyryladenosine 3′:5′-cyclic monophosphate, dbcAMP (Sigma-Aldrich). The oocytes were microinjected with RNA samples (0.2 μg/μl), 4 mM morpholino oligonucleotide (MO; Gene Tools, Philomath, OR, see Table 1), or 50 mM small interfering RNA (siRNA; Sigma-Aldrich, see Table 1) using a FemtoJet constant flow system (Eppendorf, Hamburg, Germany). The oocytes were cultured in KSOM medium (SOM with a higher K^+ concentration) containing 5% BSA at 37°C under 5% CO_2 in air.

Immunoblot analysis

Proteins were separated by SDS-PAGE and transferred onto Immobilon-P polyvinylidene difluoride membranes (Millipore, Bedford, MA). The blots were blocked with 20 mM Tris-HCl, pH 7.5, containing 5% skim milk, 0.1% Tween-20, and 0.15 M NaCl, incubated with primary antibodies and then treated with secondary antibodies conjugated with horseradish peroxidase. The immunoreactive proteins were visualized using an ECL or ECL Prime Western

Table 1

MO	Gene	Name	Sequence (5'-3')
	Mos	Mos/MO	CACAGGCTTAGAGGCGAAGGCATT
	Emi2	EMI2/MO	ATTGCTTCCTGCTCTGTGGCTGGCT

siRNA	Gene	Name	Sequence (5'-3')
	Erk1	ERK1-1 (sense)	CAUGAGAGAUGUUUACAUUTT
	Erk1	ERK1-1 (anti sense)	AAUGUAAACAUCUCUCAUGTT
	Erk1	ERK1-2 (sense)	CUGGCUUUCUGACGGAGUATT
	Erk1	ERK1-2 (anti sense)	UACUCCGUCAGAAAGCCAGTT
	Erk1	ERK1-3 (sense)	CCCAAACAAGCGCAUCACATT
	Erk1	ERK1-3 (anti sense)	UGUGAUGCGCUUGUUUGGGTT
	Erk2	ERK2-1 (sense)	AGUAUAUCCAUUCAGCUAATT
	Erk2	ERK2-1 (anti sense)	UUAGCUGAAUGGAUAUACUTT
	Erk2	ERK2-2 (sense)	GGAAGAUCUGAAUUGUAUATT
	Erk2	ERK2-2 (anti sense)	UAUACAAUUCAGAUCUUCCTT
	Erk2	ERK2-3 (sense)	GAAAUUAUGUUGAAUUCCATT
	Erk2	ERK2-3 (anti sense)	UGGAAUUCAACAUAAUUUCTT
	p38	p38-1 (sense)	UGCGUCUGCUGAAGCACAUTT
	p38	p38-1 (anti sense)	AUGUGCUUCAGCAGACGCATT
	p38	p38-2 (sense)	CCCUUAUGACCAGUCCUUUTT
	p38	p38-2 (anti sense)	AAAGGACUGGUCAUAAGGGTT
	p38	p38-3 (sense)	CGUUUCAGUCCAUCAUUCATT
	p38	p38-3 (anti sense)	UGAAUGAUGGACUGAAACGTT

MO, morpholino oligonucleotide; siRNA, small interfering RNA

Blotting Detection kit (GE Healthcare, Piscataway, NJ).

Immunostaining analysis

Oocytes were fixed in phosphate-buffered saline (PBS) containing 4% paraformaldehyde at 4°C for 2 h, treated with 1% Triton X-100 in PBS for 20 min, and blocked with PBS containing 1.5% goat serum and 0.05% Tween-20 at room temperature for 60 min. The oocytes were incubated with FITC-conjugated anti-α-tubulin antibody at room temperature for 60 min, counterstained with Hoechst 33342, and then viewed under an IX71 fluorescence microscope (Olympus, Tokyo, Japan), as previously described (Kimura et al., 2009).

RNA synthesis in vitro

RNAs were synthesized by T7 polymerase using a RiboMAX Large Scale RNA Production System-T7 kit (Promega, Madison, WI). The synthesized RNAs were treated with RQ1 RNase-free DNase (Promega) at 37ºC for 20 min, extracted with phenol-chloroform, precipitated with ethanol, dissolved in 10 mM Tris-HCl, pH 7.4, containing 0.1 mM EDTA, applied to MicroSpin G-25 columns (GE Healthcare), and stored at -80°C.

Immunoprecipitation

HEK293T cells were cultured in Dulbecco-modified Eagle medium supplemented with 10% fetal bovine serum, 100 U/ml of penicillin, and 0.1 mg/ml of streptomycin at 37°C under 5% CO_2 in air. Cells were transfected with expression plasmids encoding FLAG-HA-tagged MSK1, using a PerFectin transfection reagent (Genlantis, San Diego, CA). After 48 h, cells were cultured in serum-free medium for 24 h and then treated with 1 μM 12-*O*-tetradecanoylphorbol-13-acetate (TPA; LC Laboratories, Woburn, MA) for 60 min. Cells were lysed in a lysis buffer containing 25 mM Tris-HCl, pH 7.5, 0.15 M NaCl, 0.1% SDS, 1% NP-40, 1 mM EDTA, 1 μg/ml aprotonin, 1 μg/ml pepstatin, 1 μg/ml leupeptin, 50 μg/ml PMSF, 1 mM DTT, 20 mM NaF, and 0.5 mM Na_3VO_4. The cell lysates were subjected to immunoprecipitation using anti-FLAG M2-agarose beads (Sigma-Aldrich).

RNA interference

NIH3T3 cells were transfected with siRNA (0.1 μM) using Lipofectamine 2000 (Invitrogen, Carlsbad, CA). After 24 h, cells were treated with 10 μM or 0.5 mM H_2O_2 for 60 min for oxidative stress, and then lysed with the above lysis buffer. Proteins in the cell lysates were subjected to immunoblot analysis.

In vitro kinase assay

In vitro kinase assays were carried out in 10 mM Tris-HCl, pH 7.5, containing 10 mM $MgCl_2$, 0.1 mM DTT, 2 mM Na_3VO_4, 50 μM NaF, and 0.2

mM ATP. GST-tagged EMI2 protein (1 μg) was incubated with MSK1 purified from HEK293T cells, MNK1 (Life Technologies, Carlsbad, CA), or MK2 (Enzo Life Sciences, Farmingdale, NY) in the above buffer at 30°C for 30 min, and analyzed by immunoblotting using anti-phosphorylated EMI2 antibody.

Statistical analysis

Data are presented as mean values ± S.E. (n = 3 or 4). The Student's t-test was used for statistical analysis; significance was assumed for $p < 0.05$.

RESULTS

Possible involvement of Mos in phosphorylation of p38

I initially examined whether phosphorylation of p38 was affected by depletion of Mos. Since MO is known to effectively induce Mos reduction (Coonrod et al., 2001), GV-stage oocytes were injected with 4 mM MO against *Mos* mRNA (Mos/MO) or 4 mM negative control MO (Control/MO) in FHM containing dbcAMP. After 2-h incubation, the oocytes were cultured in KSOM medium in the absence of dbcAMP for 16 h. Depletion of Mos was verified by immunoblot analysis (Fig. 13A). Importantly, phosphorylation of both ERK1/2 and p38 was remarkably decreased in the Mos-depleted oocytes. Immunostaining analysis indicated that approximately 70% of the Control/MO-injected oocytes were arrested at metaphase II, whereas a significantly low proportion (15%) of the metaphase-II oocytes was found in the Mos/MO-injected oocytes (Fig. 13B). Since almost 60% of the Mos/MO-injected oocytes contained large polar bodies or decondensed chromatin formation, as described previously (Coonrod et al., 2001), the oocytes exhibiting abnormal cell divisions were classified into other cell-cycle stage. These results suggest that Mos may be involved in the phosphorylation state of p38, and imply that p38 may partly participate in the metaphase-II arrest.

p38 contributes to metaphase-II arrest

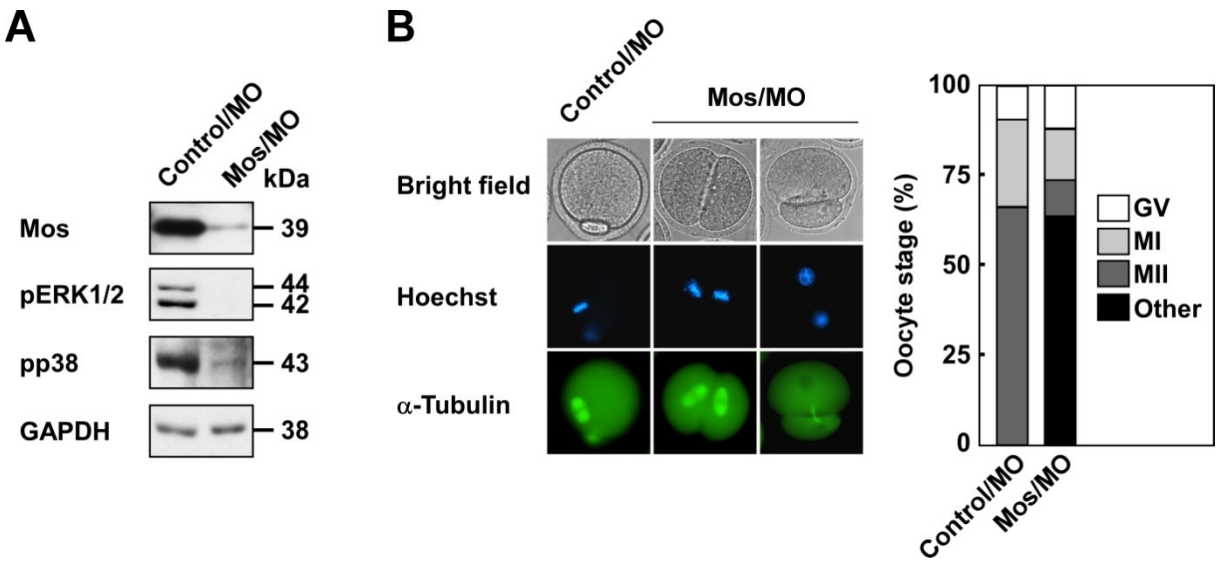

Fig. 13. Possible involvement of Mos in phosphorylation of p38. (A) Depletion of Mos by injection with morpholino oligonucleotide (MO). The germinal vesicle (GV)-stage oocytes were injected with 4 mM MO against *Mos* mRNA (Mos/MO) or negative control MO (Control/MO), and incubated in the presence of dbcAMP. After 2-h incubation, the oocytes were cultured in the absence of dbcAMP for 16 h. Whole protein extracts of the MO-injected oocytes (30 cells/lane) were analyzed using antibodies against Mos, phosphorylated ERK1/2 (pERK1/2), phosphorylated p38 (pp38), and GAPDH. (B) Immunostaining analysis. The injected oocytes were stained with α-tubulin (green) and Hoechst 33342 (blue). The ratio of oocytes at the GV, metaphase I (MI), metaphase II (MII), and other stages was counted.

To test the possibility that a p38 pathway functions in metaphase-II arrest, I examined the effect of U0126 and SB203580 (Favata et al., 1998; Frantz et al., 1998) that specifically interfere with the activity of MEK1/2 and p38, respectively (Fig. 14). Themetaphase-II oocytes were incubated with 20 μM U0126 and/or 60 μM SB203580 for 7 h, and subjected to immunostaining analysis (Fig. 14A). SB203580 had little effect on the metaphase-II arrest (Fig. 14B). Approximately 20% of the U0126-treated oocytes exhibited cell-cycle resumption, and the remainder (~80%) maintained the arrest with shrinking bipolar spindle. The simultaneous treatment with U0126 and SB203580 led to chromosome segregation, a hallmark of anaphase progression (~90% of the total oocytes). Although the level of cyclin B1 slightly decreased in the presence of U0126 or SB203580, simultaneous treatment dramatically induced degradation of cyclin B1 (Fig. 14C). Moreover, the phosphorylation state of ERK1/2 was not affected by SB203580, as expected. Thus, the p38 pathway, in addition to the Mos-MAPK pathway, may contribute to the maintenance of metaphase-II arrest.

Phosphorylation of EMI2 in mouse oocytes

Xenopus Emi2 is activated and stabilized by phosphorylation at S335, T336, S342 and S344 during meiosis II (Inoue et al., 2007; Nishiyama et al., 2007). These four Ser/Thr residues are evolutionarily well conserved in the mouse, human, and zebrafish counterparts (Fig. 15A). To examine phosphorylation of EMI2 by the p38 pathway, I prepared anti-phosphorylated EMI2 antibody that recognizes phosphorylated S326 and T327 of mouse EMI2. The antibody specificity was validated by in vitro kinase assays using MSK1 purified from

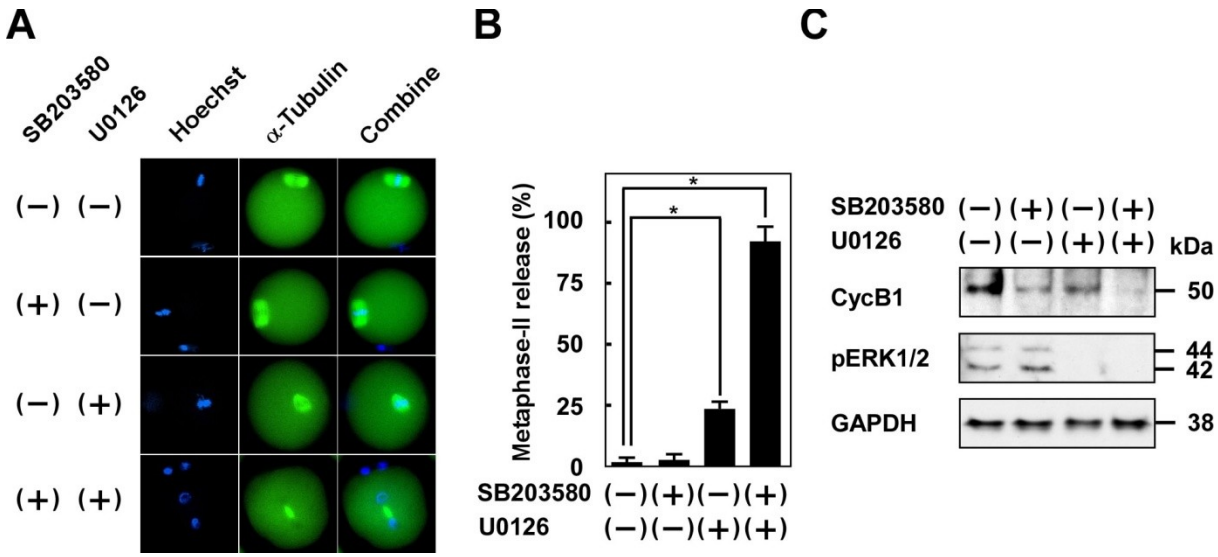

Fig. 14. p38 contributes to metaphase-II arrest. **(**A) Immunostaining analysis. The metaphase-II oocytes were incubated in the absence (−) or presence (+) of 60 μM SB203580 and 20 μM U0126 for 7 h and stained with anti-α-tubulin antibody (green) and Hoechst 33342 (blue). (B) The effect of SB203580 and U0126 on metaphase-II release. The metaphase-II oocytes were incubated in the absence (−) or presence (+) of 60 μM SB203580 and 20 μM U0126 for 7 h. The ratio of oocytes released from metaphase-II arrest was counted (*p<0.05). (C) Immunoblot analysis. The metaphase-II oocytes were incubated with (+) or without (−) 60 μM SB203580 and 20 μM U0126 for 7 h. Whole protein extracts (30 cells/lane) were analyzed using anti-cyclin B1 (CycB1), anti-phosphorylated ERK1/2 (pERK1/2), and anti-GAPDH antibodies.

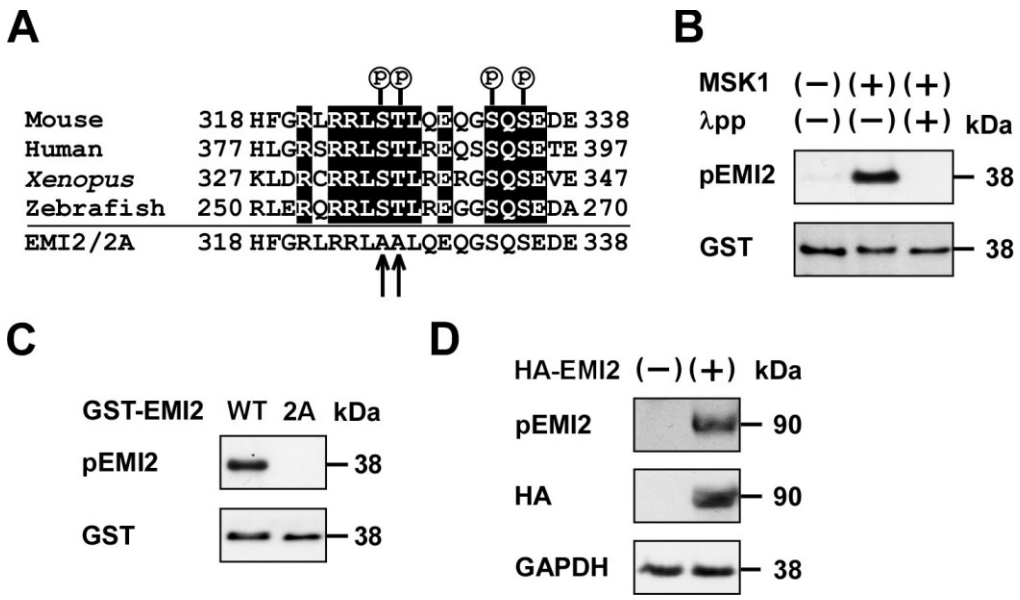

Fig. 15. Phosphorylation of EMI2 in mouse oocytes. **(**A) Alignment of the amino acid sequences of EMI2 among mouse, human, *Xenopus*, and zebrafish. Black boxes indicate the conserved residues. S326, T327, S333, and S335 of mouse EMI2 are phosphorylated by MSK1 and RSKs. The sequence of an EMI2/2A mutant is also aligned. (B) In vitro kinase assay. GST-tagged EMI2 was incubated with (+) or without **(−)** 100 ng purified MSK1, treated with (+) or without **(−)** lambda protein phosphatase (λpp), and subjected to immunoblot analysis using anti-phosphorylated EMI2 (pEMI2) and anti-GST antibodies. (C) Recognition of EMI2/2A by anti-pEMI2 antibody. GST-tagged wild-type EMI2 (WT) or EMI2/2A (2A) was incubated with (+) or without **(−)** MSK1. (D) Phosphorylation of EMI2 in mouse oocytes. The GV-stage oocytes were injected with (+) polyadenylated RNA encoding HA-tagged EMI2/DSG or were not injected **(−);** these oocytes were cultured for 12 h. The injected oocytes (15 cells/lane) were subjected to immunoblot analysis using antibodies against pEMI2, HA, and GAPDH.

HEK 293T cells and GST-fused protein containing the amino acid sequence of EMI2 at positions 288-383. Consistent with the fact that MSK1 phosphorylates S326, T327, S333, and S335 in the EMI2 peptide (Miyagaki et al., 2011), MSK1-phosphorylated EMI2 was recognized by anti-phosphorylated EMI2 antibody (Fig. 15B). No protein was immunoreactive with anti-phosphorylated EMI2 antibody, when phosphorylated EMI2 was treated with lambda protein phosphatase (Fig. 15B), and when a GST-fused EMI2 mutant protein, EMI2/2A, in which S326 and T327 are substituted with Ala (Miyagaki et al., 2011), was analyzed by in vitro kinase assays (Fig. 15C). Thus, this antibody recognizes S326- and T327-phosphorylated EMI2. To ascertain phosphorylation of EMI2 in mouse oocytes, I carried out immunoblot analysis of metaphase-II oocytes using anti-phosphorylated EMI2 antibody. However, no phosphorylated EMI2 immunoreactive with the antibody was found when 50 metaphase-II oocytes were examined (data not shown). The reason may be due to a very low abundance of EMI2 in the metaphase-II oocytes. I thus injected RNA encoding an HA-tagged EMI2 mutant, EMI2/DSG (Miyagaki et al., 2011), into GV-stage oocytes, because the mutant protein is thought to be resistant to a ubiquitin-mediated proteolysis (Shoji et al., 2006). The EMI2/DSG-injected oocytes were cultured for 12 h and subjected to immunoblot analysis (Fig. 15D). The exogenous phosphorylated EMI2 was detected as a 90-kDa protein. These results suggest that the mouse oocytes possess an effective tool for phosphorylation of EMI2.

Phosphorylation of EMI2 by the p38 pathway

At least five Ser/Thr kinases have been identified as substrates of p38 (Cargnello and Roux, 2011). I speculated that these five kinases are involved in phosphorylation of EMI2. To ask whether EMI2 is targeted by the p38 pathway in the CSF arrest, HA-tagged EMI2/DSG RNA was injected into GV-stage oocytes in the presence of dbcAMP. The EMI2/DSG-injected oocytes were then cultured in the absence of dbcAMP for 12 h, and the oocytes were further transferred to a medium containing U0126 and/or SB203580 (Fig. 16A). SB203580 had little effect on phosphorylation of EMI2, whereas EMI2 phosphorylation was approximately 30% inhibited by the presence of U0126 (Fig. 16B). A significantly great reduction (~70%) of EMI2 phosphorylation was induced by simultaneous treatment with U0126 and SB203580. Thus, EMI2 phosphorylation may be coregulated by the p38 pathway, in addition to the MEK1/2 pathway. Exogenously expressed *Emi2* in the GV-stage oocytes is known to induce the metaphase-I arrest under the above conditions (Suzuki et al., 2010; Miyagaki et al., 2011). To examine whether the metaphase-I arrest is released by kinase inhibitors, I performed immunostaining analysis of inhibitor-treated oocytes (Fig. 16C). The bipolar spindle with chromosome alignment was normally observed after the treatment with each of U0126 and SB203580, indicating the maintenance of metaphase-I arrest. Despite significantly reduced phosphorylation of EMI2, the oocytes treated with both U0126 and SB203580 underwent no chromosome segregation but contained irregularly scattered chromosomes.

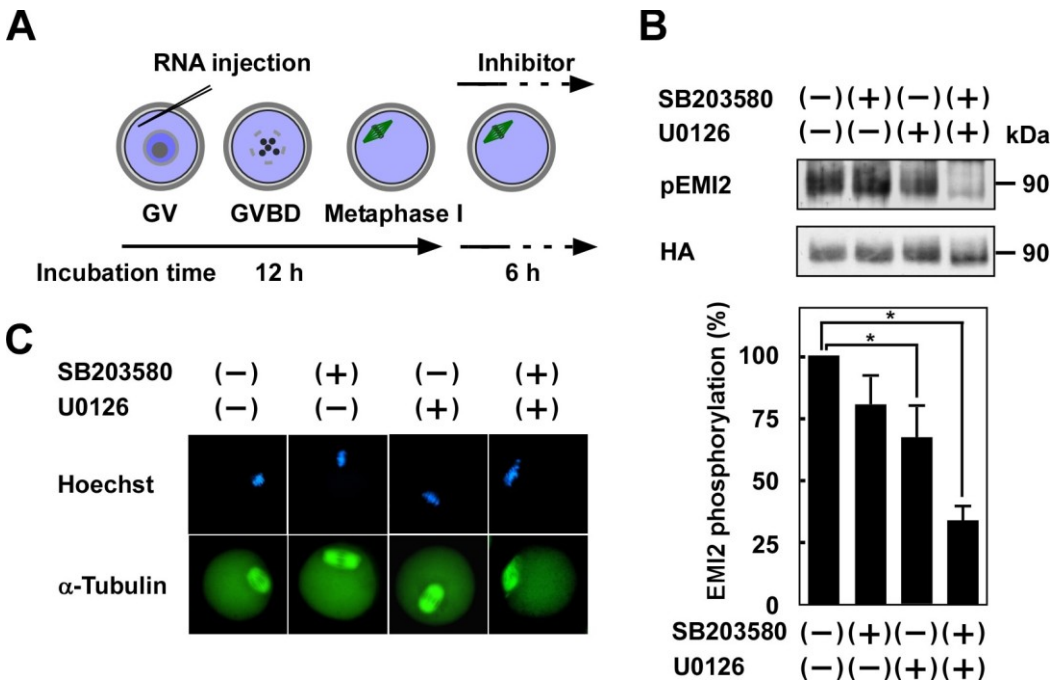

Fig. 16. p38 pathway is involved in phosphorylation of EMI2. **(**A) Experimental protocol for expression of HA-tagged EMI2/DSG mutant. The germinal vesicle (GV)-stage oocytes were injected with polyadenylated RNA encoding HA-tagged EMI2/DSG in the presence of dbcAMP and cultured in the absence of dbcAMP for 12 h. After 12 h of culture, the oocytes were incubated in the presence of kinase inhibitors for 6 h. GVBD, GV breakdown. (B) Immunoblot analysis. The injected oocytes were incubated in the absence (−) or presence (+) of 60 μM SB203580 and 20 μM U0126 for 6 h. The whole protein extracts (30 cells/lane) were subjected to immunoblot analysis using antibodies against phosphorylated EMI2 (pEMI2) and HA. Chemiluminescence intensity of pEMI2 was measured and corrected by HA intensity (*p<0.05). (C) Immunostaining analysis. The injected oocytes were incubated with (+) or without (−) 60 μM SB203580 and 20 μM U0126 for 6 h, stained with anti-α-tubulin antibody (green) and counterstained with Hoechst 33342 (blue).

Direct phosphorylation of EMI2 by MNK1

Since MNK1 and MK2 as substrates of p38 are activated during oocyte maturation (Ellederová et al., 2008; Yuan et al., 2010), I asked if these two kinases directly phosphorylate EMI2. In vitro kinase assays indicated that both MNK1 and MK2 are capable of phosphorylating EMI2 (Figs. 17A and 17B). I also examined the effects of two kinase inhibitors, CGP57380 and CMPD1, on the phosphorylation state of EMI2 in mouse oocytes (Fig. 17C). CGP57380 is known to inhibit the activity of MNK1 and exhibit no inhibitory effect on p38 and ERK1/2 (Knauf et al., 2001). On the other hand, p38-catalyzed phosphorylation of MK2 is inhibited by CMPD1 in a non-ATP-competitive manner; this inhibitor specifically blocks the p38 activity toward MK2 (Davidson et al., 2004). The GV-stage oocytes were injected with HA-tagged EMI2/DSG RNA, matured to the metaphase-I stage, and then incubated in the presence of 20 μM U0126 and 60 μM CGP57380 or 60 μM CMPD1 for 6 h. HA-tagged EMI2 remained phosphorylated in the oocytes treated with U0126 and CMPD1, whereas the treatment with both U0126 and CGP57380 inhibited phosphorylation of EMI2. Moreover, CGP57380 alone had little effect on phosphorylation of EMI2 (Fig. 18). These data suggest that MNK1, in addition to other kinases downstream of MEK1/2, phosphorylates EMI2 during the CSF arrest. Phosphorylation of MNK1 at positions T197 and T202 by ERK1/2 and p38, respectively, are required for the activity of MNK1 in somatic cells (Fukunaga and Hunter, 1997; Waskiewicz et al., 1997). I examined whether MNK1 phosphorylation in the oocytes depends on ERK1/2 and p38. When the

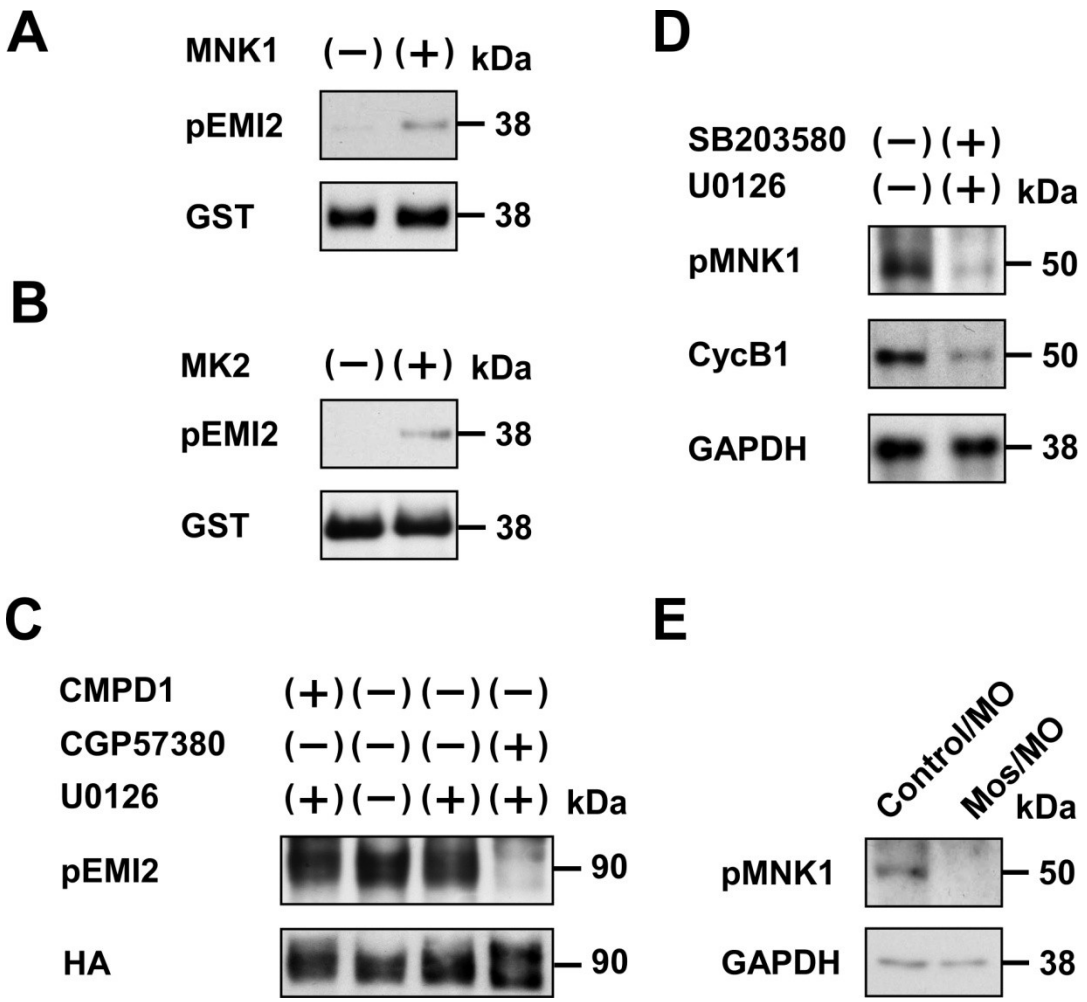

Fig. 17. Direct phosphorylation of EMI2 by MNK1. (A and B) In vitro kinase assays for phosphorylation of EMI2 by MNK1 and MK2. GST-tagged EMI2 was incubated with (+) or without (−) 350 ng MNK1 or 100 ng MK2 and subjected to immunoblot analysis using anti-phosphorylated EMI2 (pEMI2) and anti-GST antibodies. (C) Effect of CMPD1 and CGP57380 on EMI2 phosphorylation in the oocytes. The germinal vesicle (GV)-stage oocytes were injected with RNA encoding HA-tagged EMI2/DSG in the presence of dbcAMP and cultured in the absence of dbcAMP for 12 h. The oocytes (30 cells/lane) were incubated in the absence (−) or presence (+) of 60 μM CMPD1, 60 μM CGP57380, or 20 μM U126 and were subjected to immunoblot analysis using antibodies against pEMI2 and HA. (D) The effect of SB203580 and U0126 on the phosphorylation of MNK1. The metaphase-II oocytes (30 cells/lane) were incubated with (+) or without (−) 60 μM SB203580 and 20 μM U0126 for 7 h and subjected to immunoblot analysis using anti-phosphorylated MNK1 (pMNK1), anti-cyclin B1 (CycB1), and anti-GAPDH antibodies. (E) Mos regulates phosphorylation of MNK1. The GV-stage oocytes were injected with 4 mM morpholino oligonucleotide (MO) against *Mos* mRNA (Mos/MO) or negative control MO (Control/MO) and incubated in the presence of dbcAMP. After 2-h incubation, the oocytes (30 cells/lane) were cultured in the absence of dbcAMP for 16 h and subjected to immunoblot analysis using anti-pMNK1 and anti-GAPDH antibodies.

metaphase-II oocytes were treated with both SB203580 and U0126 for 6 h, the level of phosphorylated MNK1 was remarkably decreased (Fig. 17D). The injection of Mos/MO into the GV-stage oocytes also induced downregulation of phosphorylated MNK1 (Fig. 17E).

Thus, phosphorylation of MNK1 may be regulated by the Mos-MAPK and p38 MAPK pathways in the metaphase-II oocytes.

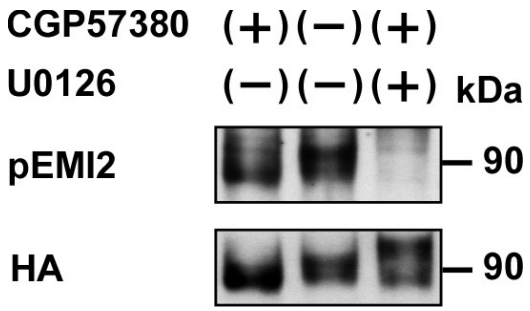

Fig. 18. Effect of CGP57380 on phosphorylation state of EMI2. The germinal vesicle (GV)-stage oocytes were injected with RNA encoding HA-tagged EMI2/DSG in the presence of dbcAMP. The injected oocytes were cultured for 12 h in the absence of dbcAMP and incubated with (+) or without (−) 60 μM CGP57380 and 20 μM U0126 for 6 h. Whole protein extracts (30 cells/lane) were subjected to immunoblot analysis using anti-phosphorylated EMI2 (pEMI2) and anti-HA antibodies.

DISCUSSION

This study reveals that p38 plays an important role in EMI2-mediated metaphase-II arrest in the mouse oocytes. Although Mos activates MEK1/2 during oocyte maturation (Nebreda and Hunt, 1993; Posada et al., 1993; Shibuya and Ruderman, 1993), Mos has been postulated to inhibit the activity of an unknown phosphatase (Verlhac et al., 2000). As shown in Fig. 13A, the inhibition of Mos synthesis results in the failure of p38 phosphorylation, suggesting that Mos may regulate phosphorylation of p38. Activation of p38 requires phosphorylation at T180 and Y182 in Thr-Gly-Tyr motif by MKK3/6 (Raingeaud et al., 1995; Enslen et al., 2000). It is unlikely that Mos directly phosphorylates p38 in the metaphase-II oocytes, because Mos is a Ser/Thr kinase incapable of phosphorylating Y182 in p38. Thus, I assume that phosphorylation of p38 is regulated by a Mos-mediated phosphatase, or that Mos regulates a kinase(s) upstream of p38.

The metaphase-II arrest was released by inhibition of MEK1/2 and p38 (Fig. 14B). Inhibition of each kinase activity was insufficient to exit from metaphase II, implying the presence of a compensatory mechanism. Since the MEK1/2-depleted oocytes develop to metaphase II and maintain the metaphase-II arrest (Yu et al., 2007), the p38 pathway may compensate for phosphorylation of EMI2 in the MEK1/2-depleted oocytes. Approximately 20% of the oocytes treated with U0126 were released from the metaphase-II arrest, whereas SB203580 had little effect (Fig. 14B). These results suggest that

phosphorylation of EMI2 may be regulated more predominantly by the Mos-MAPK pathway than by the p38 pathway.

The simultaneous treatment with U0126 and SB203580 induced ~70% reduction in phosphorylation of EMI2 in the metaphase I-arrested oocytes (Fig. 16B). Unexpectedly, the metaphase-I arrest was maintained in the presence of these two inhibitors, despite the remarkable decrease in EMI2 phosphorylation (Fig. 16C). The maintenance of metaphase-I arrest may be due to the possibility that a relatively low level (~30%) of phosphorylated EMI2 may be enough to interfere with the cell-cycle resumption. Moreover, the metaphase I-arrested oocytes displayed the abnormality in spindle formation and chromosome alignment in the presence of both SB203580 and U0126 (Fig. 16C). These results suggest that in addition to phosphorylation of EMI2, MEK1/2 and p38 may have other unique functions. Mos is indispensable for activation of MISS and DOC1R that are localized at the metaphase spindle and are involved in spindle formation (Lefebvre et al., 2002; Terret et al., 2003). My data revealed that phosphorylated p38 is colocalized with α-tubulin at the metaphases I and II (Fig. 19). Thus, the p38 pathway as well as the Mos-MAPK pathway may be implicated in spindle formation through activation of MISS and DOC1R.

It has been reported that phosphorylated MK2 is present during oocyte maturation, and CMPD1 (30 μM) is sufficient to inhibit the activity of MK2 in mouse oocytes (Yuan et al., 2010). I found that although MK2 phosphorylates EMI2 in vitro (Fig. 5B), EMI2 in mouse oocytes is barely phosphorylated even in the presence of 60 μM CMPD1 (Fig. 17C). Thus, EMI2 phosphorylation may be unaffected by MK2 in the CSF-arrested oocytes. Further experiments are

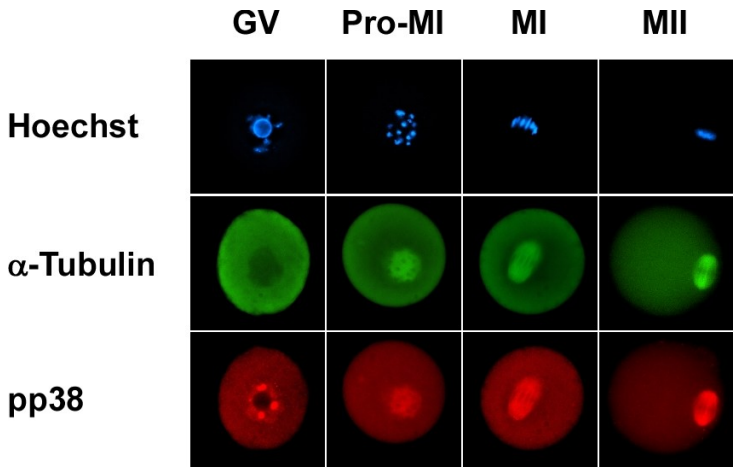

Fig. 19. Localization of phosphorylated p38 during oocyte maturation. Immunostaining analysis. The germinal vesicle (GV)-, prometaphase I (Pro-MI)-, metaphase I (MI)-, and metaphase II (MII)-stage oocytes were stained with anti-phosphorylated p38 (pp38, red) and FITC-conjugated anti-α-tubulin (green) antibodies and counterstained with Hoechst 33342 (blue).

required to elucidate the functional difference of MK2 between in vitro and in vivo.

To clarify the role of p38 and ERK1/2 in establishing the metaphase-II arrest, I designed siRNAs against the three mRNAs (Table 1). The levels of phosphorylated p38, ERK1, and ERK2 were 70~85% decreased by introduction of the siRNAs into NIH3T3 cells (Fig. 20A). In the mouse oocytes, the levels of these three kinases were unchanged by the siRNA injection (Fig. 20B). siRNA knockdown of Mos and EMI2 was enough to interfere with normal maturation of oocytes (Figs. 13 and 21). p38 and ERK1/2 are already present in the GV-stage oocytes (Ou et al., 2010; Verlhac et al., 1993), whereas Mos and EMI2 are synthesized after GV-breakdown and metaphase-I stages, respectively (Paules et al., 1989; Madgwick et al., 2006). I thus speculate that proteins already present at the GV stage are not efficiently reduced by the siRNA injection into the oocytes.

Mos has been demonstrated to trigger the MEK1/2-ERK1/2 cascade (Nebreda and Hunt, 1993; Posada et al., 1993; Shibuya and Ruderman, 1993). My results suggest that Mos may function in phosphorylation of p38 involved in activation of EMI2 through phosphorylation of MNK1. I have previously reported the functional redundancy of MSK1 and RSKs in EMI2 phosphorylation (Miyagaki et al., 2011). Since MNK1 is one of kinases that participate in phosphorylation of EMI2, the MEK1/2-ERK1/2-RSK1/2/3 or MSK1-EMI2 and p38-MNK1-EMI2 cascades governed by Mos may mediate the metaphase-II arrest in the mouse oocytes.

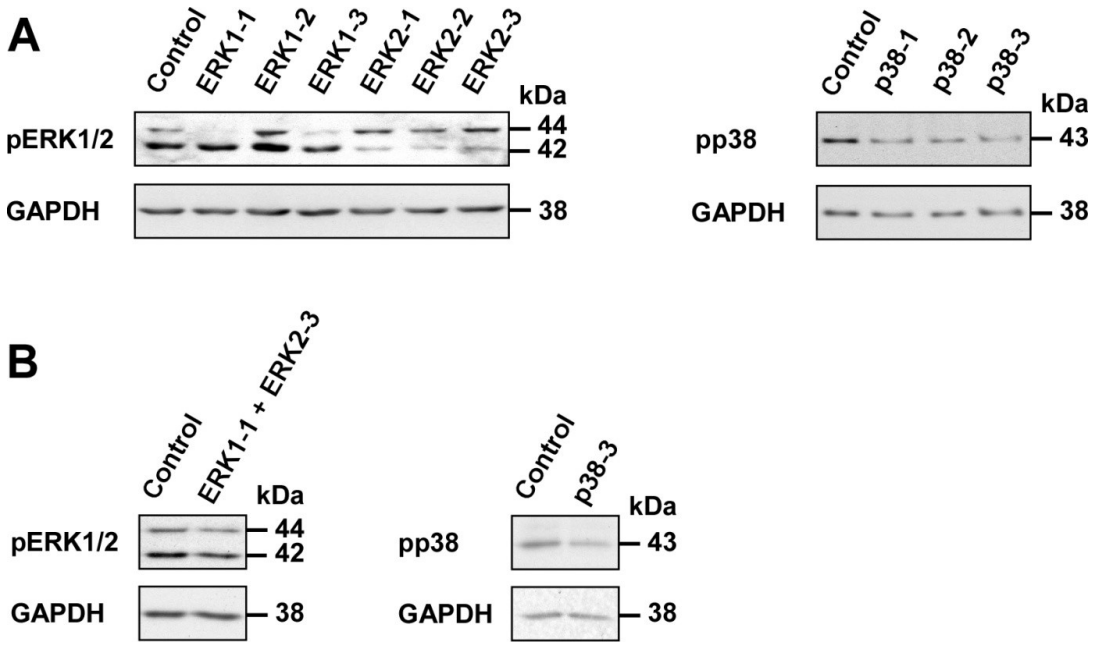

Fig. 20. RNA interference for *Erk1*, *Erk2*, and *p38*. (A) I designed three different sequences of small interfering RNA (siRNA) against each mRNA, *Erk1*, *Erk2*, and *p38* (ERK1-1/2/3, ERK2-1/2/3, and p38-1/2/3). NIH3T3 cells were transfected with the siRNAs or negative control (Control). After 24 h of culture, cells were incubated in the presence of 10 μM or 0.5 mM H_2O_2 for 60 min and subjected to immunoblot analysis using anti-phosphorylated ERK1/2 (pERK1/2), anti-phosphorylated p38 (pp38), and anti-GAPDH antibodies. (B) The germinal vesicle (GV)-stage oocytes were injected with a mixture of ERK1-1 and ERK2-3, p38-3, or Control and incubated in the presence of dbcAMP for 24 h. The injected oocytes were cultured in the absence of dbcAMP for 16 h and subjected to immunoblot analysis using antibodies against pERK1/2, pp38, and GAPDH.

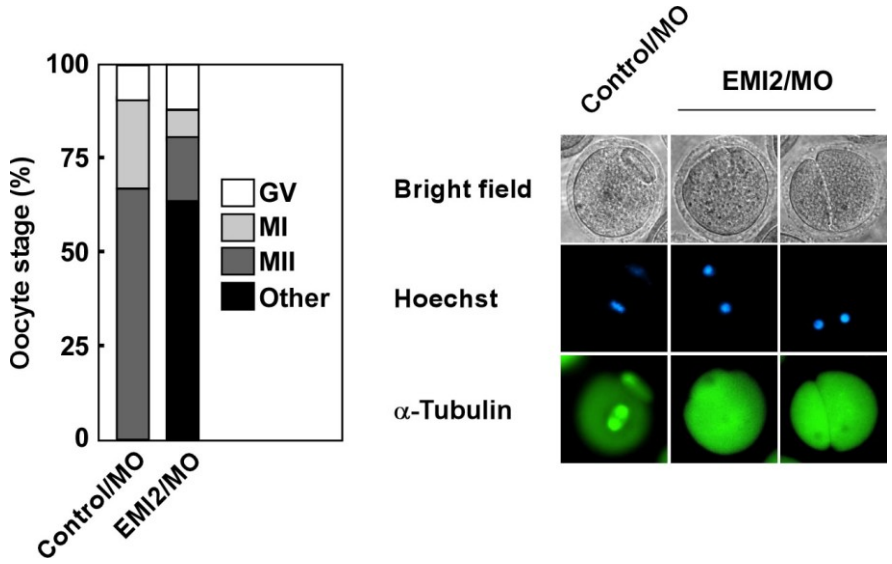

Fig. 21. EMI2 depletion by injection with morpholino oligonucleotide (MO). The germinal vesicle (GV)-stage oocytes were injected with 4 mM MO against *Emi2* mRNA (EMI2/MO) or negative control MO (Control/MO) and incubated in the presence of dbcAMP for 2 h. The oocytes were then cultured in the absence of dbcAMP for 16 h and subjected to immunostaining analysis using FITC-conjugated anti-α-tubulin antibody (green) and Hoechst 33342 (blue). The ratio of oocytes at the GV, metaphase I (MI), metaphase II (MII), and other stages was counted.

GENERAL CONCLUSION

This study raises the possibility that MSK1 and p38 contribute to maintenance of metaphase-II arrest in the mouse oocytes.

The chapter I describes the possible role of MSK1 in the oocytes. MSK1 was present during oocyte maturation, and was phosphorylated at the metaphase-I and metaphase-II stages (Figs. 2 and 10). Phosphorylated MSK1 exhibited the ability to phosphorylate EMI2 in vitro (Fig. 7). In addition, the treatment of metaphase II-arrested oocytes with the inhibitor of MSK1 released the oocytes from the metaphase-II stage (Fig. 5). Thus, MSK1 may play a key role in the metaphase-II arrest through phosphorylation of EMI2. In the chapter II, I examined whether p38 is regulated under the control of Mos and has a role in the metaphase-II arrest. Since phosphorylation of p38 was abolished by depletion of Mos (Fig. 13), Mos may be involved in p38 phosphorylation. Interestingly, the treatment of oocytes with the inhibitors of p38 and MEK1/2 revealed a remarkable decrease in phosphorylation of EMI2, and induced activation of metaphase-II oocytes (Figs. 14 and 16). These results suggest that the p38 pathway, in addition to the MEK1/2 pathway, may be implicated in the metaphase-II arrest. On basis of these data obtained, I propose a schematic model for phosphorylation of EMI2 (Fig. 22). Although Mos triggers the MEK1/2-ERK1/2 cascade (Nebreda and Hunt, 1993; Posada et al, 1993; Shibuya and Runderman, 1993), my results suggest that Mos may be involved in phosphorylation of p38 as well as MEK1/2. Moreover, it is most likely that MSK1 and MNK1 both contribute to phosphorylation of EMI2.

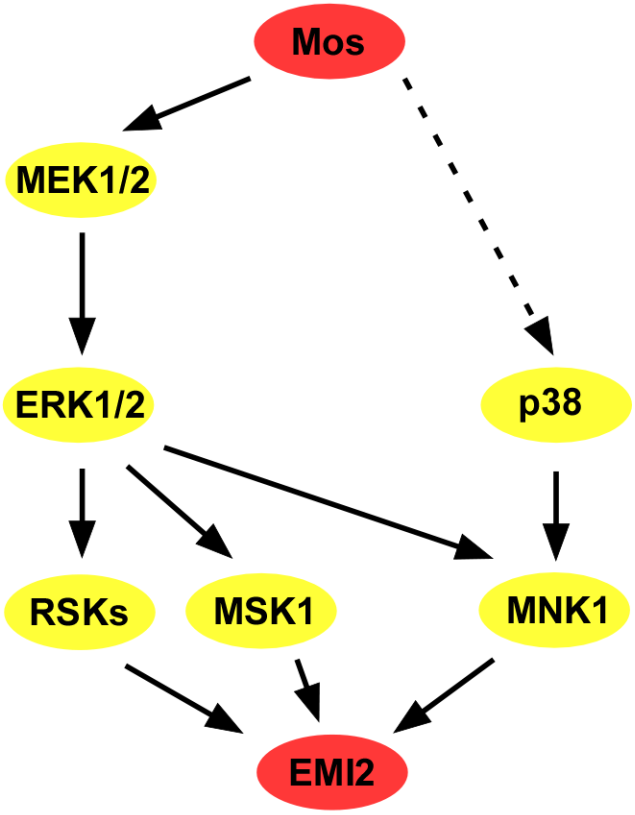

Fig. 22. A Schematic model for metaphase-II arrest in mouse oocytes. Mos may regulate the phosphorylation state of p38 as well as MEK1/2. In addition to RSKs, two Ser/Thr kinases, MSK1 and MNK1, are capable of phosphorylating EMI2. Thus, Mos governs at least two signaling pathways: MEK1/2 and p38 pathways.

Parthenogenetic activation of mouse oocytes has been suggested to result in development of ovarian teratomas (Eppig et al, 1977). Indeed, ovarian tumors develop in the Mos-defficient mouse (Furuta et al, 1995). Thus, this study will provide a clue to elucidate the mechanism of ovarian tumorigenesis.

ACKNOWLEDGEMENTS

I would like to express my gratitude to all those who offered me guidance supports and encouragement during the preparation of this doctoral thesis.

First of all, I would like to express my sincere appreciation to Professor Tadashi Baba for all his supports and guidance throughout my research work. I wish to express my deep thanks to Dr. Yoshinori Kanemori for his support and encouragement. I also thank all members of our laboratory. Finally, I would like to give my special thanks to my father and mother.

REFERENCES

Araki, K., Naito, K., Haraguchi, S., Suzuki, R., Yokoyama, M., Inoue, M., Aizawa, S., Toyoda, Y., Sato, E., 1996. Meiotic abnormalities of c-*mos* knockout mouse oocytes: Activation after first meiosis or entrance into third meiotic metaphase. Biol Reprod. 55, 1315-1324.

Baba, T., Niida, Y., Michikawa, Y., Kashiwabara, S., Kodaira, K., Takenaka, M., Kohno, N., Gerton, G.L., Arai, Y., 1994. An acrosomal protein protein, sp32, in mammalian sperm is a binding protein specific for two proacrosins and an acrosin intermediate. J. Biol. Chem. 269, 10133-10140.

Bhatt, R.R., Ferrell, J.E.Jr., 2000. Cloning and characterization of *Xenopus* Rsk2, the predominant p90 Rsk isozyme in oocytes and eggs. J. Biol. Chem. 275, 32983-32990.

Brami-Cherrier, K., Roze, E., Girault, J.A., Betuing, S., Caboche, J., 2009. Role of the ERK/MSK1 signalling pathway in chromatin remodelling and brain responses to drugs of abuse. J. Neurochem. 108, 1323-1335.

Chang, H.Y., Minahan, K., Merriman, J.A., Jones, K.T., 2009. Calmodulin-dependent protein kinase gamma 3 (CamKIIgamma3) mediates the cell cycle resumption of metaphase II eggs in mouse. Development 136, 4077-4081

Cargnello, M., Roux, P. P., 2011. Activation and function of the MAPKs and their substrates, the MAPK-activated protein kinases. Mol. Biol. Rev. 75, 50-83.

Choi, T., Fukasawa, K., Zhou, R., Tessarollo, L., Borror, K., Resau, J., Vande Woude, G. F., 1996. The Mos/mitogen-activated protein kinase (MAPK) pathway regulates the size and degradation of the first polar body in maturing mouse oocytes. Proc. Natl. Acad. Sci. U. S. A. 93, 7032-7035.

Colledge, W. H., Carlton, M. B. L., Udy, G. B., Evans, M. J., 1994. Disruption of c-*mos* causes parthenogenetic development of unfertilized mouse eggs. Nature. 370, 65-68.

Coonrod, S. A., Bolling, L. C., Wright, P. W., Visconti, P. E., Herr, J. C., 2001. A morpholino phenocopy of the mouse mos mutation. Genesis. 30, 198-200.

Davidson, W., Frego, L., Peet, G. W., Kroe, R. R., Labadia, M. E., Lukas, S. M., Snow, R. J., Jakes, S., Grygon, C. A., Pargellis, C., Werneburg, B. G., 2004. Discovery and characterization of a substrate selective p38α inhibitor. Biochemistry. 43, 11658-11671.

Davies, S.P., Reddy, H., Caivano, M., Cohen, P., 2000. Specificity and mechanism of action of some commonly used protein kinase inhibitors. Biochem. J. 351, 95-105.

Dupré, A., Jesses, C., Ozon, R., Haccard, O., 2002. Mos is not required for the initiation of meiotic maturation in *Xenopus* oocytes. EMBO J. 21, 4026-4036.

Deak, M., Clifton, A.D., Lucocq, L.M., Alessi, D.R., 1998. Mitogen- and stress-activated protein kinase-1 (MSK1) is directly activated by MAPK and SAPK2/p38, and may mediate activation of CREB. EMBO J. 17, 4426-4441.

Dumont, J., Umbhauer, M., Rassinier, P., Hanauer, A., Verlhac, M.H., 2005.

p90Rsk is not involved in cytostatic factor arrest in mouse oocytes. J. Cell Biol. 169, 227-231.

Ellederová, Z., Cais, O., Šušor, A., Uhlířová, K., Kovářová, H., Jelínková, L., Tomek, W., Kubelka, M., 2008. ERK1/2 Map kinase metabolic pathway is Responsible for phosphorylation of translation initiation factor eIF4E during in vitro maturation of pig oocytes. Mol Reprod Dev. 75, 309-317.

Enslen, H., Brancho, D. M., Davis, R. J., 2000. Molecular determinants that mediate selective activation of p38 MAP kinase isoforms. EMBO J. 19, 1301-1311.

Eppig, J.J., Kozak, L.P., Eicher, E.M., Stevens, L.C., 1977. Ovarian teratomas in mice are derived from oocytes that have completed the first meiotic division. Nature. 269, 517-518.

Espino, P.S., Li, L., He, S., Yu, J., Davie, J.R., 2006. Chromatin modification of the trefoil factor 1 gene in human breast cancer cells by the Ras/mitogen-activated protein kinase pathway. Cancer Res. 66, 4610-4616.

Fan, H.Y., Liu, Z., Shimada, M., Sterneck, E., Johnson, P.F., Hedrick, S.M., Richards, J.S., 2009. MAPK3/1 (ERK1/2) in ovarian granulosa cells are essential for female fertility. Science 324, 938-941.

Favata, M. F., Horiuchi, K. Y., Manos, E. J., Daulerio, A. J., Stradley, D. A., Feeser, W. S., Van Dyk, D. E., Pitts, W. J., Earl, R. A., Hobbs, F., Copeland, R. A., Magolda, R. L., Scherle, P. A., Trzaskos, J. M., 1998. Identification of a novel inhibitor of mitogen-activated protein kinase kinase. J. Biol. Chem. 273, 18623-18632.

Frantz, B., Klatt, T., Pang, M., Parsons, J., Rolando, A., Williams, H., Tocci, M. J., O'Keefe, S. J., O'Neill, E. A., 1998. The activation state of p38 mitogen-activated protein kinase determines the efficiency of ATP competition for pyridinylimidazole inhibitor binding. Biochemistry. 37, 13846-13853.

Fukunaga, R., Hunter, T., 1997. MNK1, a new MAP kinase-activated protein kinase, isolated by a novel expression screening method for identifying protein kinase substrates. EMBO J. 16, 1921-1933.

Furuta, Y., Shigetani, Y., Takeda, N., Iwasaki, K., Ikawa, Y., Aizawa, S., 1995. Ovarian teratomas in mice lacking the protooncogene *c-mos*. Jpn. J. Cancer Res. 86, 540-545.

Gautier, J., Minshull, J., Lohka, M., Glotzer, M., Hunt, T., Maller, J. L., 1990. Cyclin is a component of maturation-promoting factor from *Xenopus*. Cell. 60, 487-494.

Gross, S. D., Schwab, M. S., Taieb, F. E., Lewellyn, A. L., Qian, Y. W., Maller, J. L., 2000. The critical role of the MAP kinase pathway in meiosis II in *Xenopus* oocytes is mediated by $p90^{Rsk}$. Curr. Biol. 10, 430-438.

Hashimoto, N., Watanabe, N., Furuta, Y., Tamemoto, H., Sagata, N., Yokoyama, M., Okazaki, K., Nagayoshi, M., Takeda, N., Ikawa, Y., Aizawa S., 1994. Parthenogenetic activation of oocytes in c-*mos*-deficient mice. Nature. 370, 68-71.

Hauge, C., Frodin, M., 2006. RSK and MSK in MAP kinase signalling. J. Cell Sci. 119, 3021-3023.

Inoue, D., Ohe, M., Kanemori, Y., Nobui, T., Sagata, N., 2007. A direct link of

the Mos-MAPK pathway to Erp1/Emi2 in meiotic arrest of *Xenopus laevis* eggs. Nature. 446, 1100-1104.

Kalab, P., Kubiak, J.Z., Verlhac, M.H., Colledge, W.H., Maro, B., 1996. Activation of p90rsk during meiotic maturation and first mitosis in mouse oocytes and eggs: MAP kinase-independent and -dependent activation. Development 122, 1957-1964.

Kawaguchi, M., Fujita, J., Kokubu, F., Huang, S.K., Homma, T., Matsukura, S., Adachi, M., Hizawa, N., 2009. IL-17F-induced IL-11 release in bronchial epithelial cells via MSK1-CREB pathway. Am. J. Physiol. Lung Cell Mol. Physiol. 296, L804-1810.

Kim, E., Baba, D., Kimura, M., Yamashita, M., Kashiwabara, S., Baba, T., 2005. Identification of hyaluronidase, Hyal5, involved in penetration of mouse sperm through cumulus mass. Proc. Natl. Acad. Sci. USA 102, 18028-18033.

Kimura, M., Kim, E., Kang, W., Yamashita, M., Saigo, M., Yamazaki, T., Nakanishi, T., Kashiwabara, S., Baba, T., 2009. Functional roles of sperm hyaluronidase, Hyal5 and SPAM1, in fertilization in mice. Biol. Reprod. 81, 939-947.

Kishimoto, T., 2003. Cell-cycle control during meiotic maturation. Curr. Opin. Cell Biol. 15, 654-663.

Knauf, U., Tschopp, C., Gram, H., 2001. Negative regulation of protein translation by mitogen-activated protein kinase-interacting kinases 1 and 2. Mol. Cell. Biol. 21, 5500-5511.

Lawitts, J.A., Biggers, J.D., 1993. Culture of preimplantation embryos. Methods Enzymol. 225, 153-164.

Lefebvre, C., Terret, M. E., Djiane, A., Rassinier, P., Maro, B., Verlhac, M. H., 2002. Meiotic spindle stability depends on MAPK-interacting and spindle-stabilizing protein (MISS), a new MAPK substrate. J Cell Biol. 157, 603-613.

Madgwick, S., Hansen, D. V., Levasseur, M., Jackson, P. K., Jones, K. T., 2006. Mouse Emi2 is required to enter meiosis II by reestablishing cyclin B1 during interkinesis. J. Cell Biol. 174, 791-801.

Masui, Y., Markert, C. L., 1971. Cytoplasmic control of nuclear behavior during meiotic maturation of frog oocytes. J. Exp. Zool. 177, 129-145.

Miyagaki, Y., Kanemori, Y., Baba, T., 2011. Possible involvement of mitogen- and stress-activated protein kinase 1, MSK1, in metaphase-II arrest through phosphorylation of EMI2 in mouse oocytes. Dev Biol. 359, 73-81.

Nebreda, A. R., Hunt, T., 1993. The c-*mos* proto-oncogene protein kinase turns on and maintains the activity of MAP kinase, but not MPF, in cell-free extracts of *Xenopus* oocytes and eggs. EMBO J. 12, 1979-1986.

Nishiyama, T., Ohsumi, K., Kishimoto, T., 2007. Phosphorylation of Erp1 by p90rsk is required for cytostatic factor arrest in *Xenopus laevis* eggs. Nature. 446, 1096-1099.

Oh, J.S., Han, S.J., Conti, M., 2010. Wee1B, Myt1, and Cdc25 function in distinct compartments of mouse oocyte to control meiotic resumption. J. Cell Biol. 188, 199-207.

Ou, X. H., Li, S., Xu, B. Z., Wang, Z. B., Quan, S., Li, M., Zhang, Q. H., Ouyang, Y. C., Schatten, H., Xing, F. Q., Sun, Q. Y., 2010. p38α MAPK is a MTOC-associated protein regulating spindle assembly, spindle length and

accurate chromosome segregation during mouse oocyte meiotic maturation. Cell cycle. 9, 4130-4143.

Paules, R. S., Buccione, R., Moschel, R. C., Vande Woude, G. F., Eppig, J. J., 1989. Mouse *Mos* protooncogene product is present and functions during oogenesis. Proc. Natl. Acad. Sci. U. S. A. 86, 5395-5399.

Pearce, L.R., Komander, D., Alessi, D.R., 2010. The nuts and bolts of AGC protein kinases. Nat. Rev. Mol. Cell Biol. 11, 9-22.

Perry, A.C., Verlhac, M.H., 2008. Second meiotic arrest and exit in frogs and mice. EMBO Rep. 9, 246-251.

Peters, J. M., 2006. The anaphase promoting complex/cyclosome: a machine designed to destroy. Nat Rev Mol Cell Biol. 7, 644-656.

Posada, J., Yew, N., Ahn, N. G., Vande Woude, G. F., Cooper, J. A., 1993. Mos stimulates MAP kinase in *Xenopus* oocytes and activates a MAP kinase kinase in vitro. Mol. Cell. Biol. 13, 2546-2553.

Raingeaud, J., Gupta, S., Rogers, J. S., Dickens, M., Han, J., Ulevitch, R. J., Davis, R. J., 1995. Pro-inflammatory cytokines and environmental stress cause p38 mitogen-activated protein kinase activation by dual phosphorylation on tyrosine and threonine. J. Biol. Chem. 270, 7420-7426.

Sagata, N., 1996. Meiotic metaphase arrest in animal oocytes: its mechanisms and biological significance. Trends Cell Biol. 6, 22-28.

Sagata, N., Watanabe, N., Vande Woude, G. F., Ikawa, Y., 1989. The c-*mos* proto-oncogene product is a cytostatic factor responsible for meiotic arrest in vertebrate eggs. Nature. 342, 512-518.

Sasseville, M., Ritter, L.J., Nguyen, T.M., Liu, F., Mottershead, D.G., Russell,

D.L., Gilchrist, R.B., 2010. Growth differentiation factor 9 signaling requires ERK1/2 activity in mouse granulosa and cumulus cells. J. Cell Sci. 123, 3166-3176.

Schmidt, A., Duncan, P. I., Rauh, N. R., Sauer, G., Fry, A. M., Nigg, E. A., Mayer, T. U., 2005. *Xenopus* polo-like kinase Plx1 regulates XErp1, a novel inhibitor of APC/C activity. Genes Dev. 19, 502-513.

Shibuya, E. K., Ruderman, J. V., 1993. Mos induces the in vitro activation of mitogen-activated protein kinases in lysates of frog oocytes and mammalian somatic cells. Mol. Biol. Cell. 4, 781-790.

Shoji, S., Yoshida, N., Amanai, M., Ohgishi, M., Fukui, T., Fujimoto, S., Nakano, Y., Kajikawa, E., Perry, A. C. F., 2006. Mammalian Emi2 mediates cytostatic arrest and transduces the signal for meiotic exit via Cdc20. EMBO J. 25, 834-845.

Suzuki, T., Suzuki, E., Yoshida, N., Kubo, A., Li, H., Okuda, E., Amanai, M., Perry, A. C. F., 2010. Mouse Emi2 as a distinctive regulatory hub in second meiotic metaphase. Development. 137, 3281-3291.

Terret, M. E., Lefebvre, C., Djiane, A., Rassinier, P., Moreau, J., Maro, B., Verlhac, M. H., 2003. DOC1R: a MAP kinase substrate that control microtubule organization of metaphasae II mouse oocytes. Development. 130, 5169-5177.

Thornton, T. M., Rincon, M., 2009. Non-classical p38 map kinase functions: cell cycle checkpoints and survival. Int. J. Biol. Sci. 5, 44-52.

Tong, C., Fan, H.Y., Chen, D.Y., Song, X.F., Schatten, H., Sun, Q.Y., 2003. Effects of MEK inhibitor U0126 on meiotic progression in mouse oocytes:

microtubule organization, asymmetric division and metaphase II arrest. Nat. Cell Res. 13, 375-383.

Toyoda, Y., Yokoyama, M., Hoshi, T., 1971. Studies on the fertilization of mouse eggs in vitro. Jpn. J. Anim. Reprod. 16, 147-151.

Tsurumi, C., Hoffmann, S., Geley, S., Graeser, R., Polanski, Z., 2004. The spindle assembly checkpoint is not essential for CSF arrest of mouse oocytes. J. Cell Biol. 167, 1037-1050.

Tung, J. J., Hansen, D. V., Ban, K. H., Loktev, A. V., Summers, M. K., Adler III, J. R., Jackson, P. K., 2005. A role for the anaphase-promoting complex inhibitor Emi2/XErp1, a homolog of early mitotic inhibitor 1, in cytostatic factor arrest of *Xenopus* eggs. Proc. Natl. Acad. Sci. U. S. A. 102, 4318-4323.

Tunquist, B.J., Maller, J.L., 2003. Under arrest: cytostatic factor (CSF)-mediated metaphase arrest in vertebrate eggs. Genes Dev. 17, 683-710.

Yamamoto, T. M., Iwabuchi, M., Ohsumi, K., Kishimoto, T., 2005. APC/C-Cdc20-mediated degradation of cyclin B participates in CSF arrest in unfertilized *Xenopus* eggs. Dev. Biol. 279, 345-355.

Yamazaki, T., Yamagata, K., Baba, T., 2007. Time-lapse and retrospective analysis of DNA methylation in mouse preimplantation embryos by live cell imaging. Dev. Biol. 304, 409-419.

Yu, L. Z., Xiong, B., Gao, W. X., Wang, C. M., Zhong, Z. S., Huo, L. J., Wang, Q., Hou, Y., Liu, K., Liu, X. J., Schatten, H., Chen, D. Y., Sun, Q. Y., 2007. MEK1/2 regulates microtubule organization, spindle pole tethering and asymmetric division during mouse oocyte meiotic maturation. Cell Cycle. 6,

330-338.

Yuan, J., Xu, B. Z., Qi, S. T., Tong, J. S., Wei, L., Li, M., Ouyang, Y. C., Hou, Y., Schatten, H., Sun, Q. Y., 2010. MAPK-activated protein kinase 2 is required for mouse meiotic spindle assembly and kinetochore-microtubule attachment. PloS. One. 5, e11247.

Verlhac, M. H., de Pennart, H., Maro, B., Cobb, M. H., Clarke, H. J., 1993. MAP kinase becomes stably activated at metaphase and is associated with microtubule-organizing centers during meiotic maturation of mouse oocytes. Dev. Biol. 158, 330-340.

Verlhac, M. H., Kubiak, J. Z., Weber, M., Géraud, G., Colledge, W. H., Evans, M. J., Maro, B., 1996. Mos is required for MAP kinase activation and is involved in microtubule organization during meiotic maturation in the mouse. Development. 122, 815-822.

Verlhac, M. H., Lefebvre, C., Kubiak, J. Z., Umbhauer, M., Rassinier, P., Colledge, W., Maro, B., 2000. Mos activates MAP kinase in mouse oocytes through two opposite pathways. EMBO J. 19, 6065-6074

Waskiewicz, A. J., Flynn, A., Proud, C. G., Cooper, J. A., 1997. Mitogen-activated protein kinases activite the serine/threonine kinases Mnk1 and Mnk2. EMBO J. 16, 1909-1920.

Wiggin, G.R., Soloaga, A., Foster, J.M., Murray-Tait, V., Cohen, P., Arthur, J.S., 2002. MSK1 and MSK2 are required for the mitogen- and stress-induced phosphorylation of CREB and ATF1 in fibroblasts. Mol. Cell Biol. 22, 2871-2881.

Wu, J. Q., Hansen, D. V., Guo, Y., Wang, M. Z., Tang, W., Freel, C. D., Tung, J. J., Jackson, P. K., Kornbluth, S., 2007. Control of Emi2 activity and stability through Mos-mediated recruitment of PP2A. Proc. Natl. Acad. Sci. U. S. A. 104, 16564-16569.